1 # Systematic evaluation of rock mechanical behavior

2 # of chalk reservoirs in presence of variety of water

3 # compositions

4 *AUTHOR NAMES: Bizhan Zangiabadi[1]; Sina R. Gomari[2]*

5 AUTHOR ADDRESS:

6 [1] Ph.D. Candidate, Department of Petroleum Engineering, Faculty of Science and Technology,

7 University of Stavanger, Stavanger, Norway(Corresponding author). E-mail:

8 bizhan.zangiabadi@outlook.com

9 [2] Senior Lecturer, School of Science and Engineering, University of Teesside, Middlesbrough

10 TS1 3BA UK. E-mail: S.Rezaei-Gomari@tees.ac.uk

11 KEYWORDS: chalk, chemo-mechanical, saline solutions, weakening, creep rate

12 ABSTRACT:

13 Principally, the interaction between chalk surface and saline water is vital for reported

14 subsidence, formation compaction (the decline in pore fluid pressure within a solid structure and

15 increase in stress on formation rock), as well as enhanced oil recovery (EOR) in chalk reservoirs.

16 To understand the mechanisms of rock-fluid interaction and the role of specific ions in seawater,

17    rock mechanical tests combined with chemical analysis of effluents were performed on chalk

18    outcrops using synthetic brine solutions. All the chalk cores are treated with strictly aqueous

19    solution meaning no hydrocarbon involved in any stage of experiments from preparation to post-

20    processing (chemical analysis). The two objectives in the present study are the examination of

21    diffusion and transport-controlled phenomena in the presence of different aqueous chemistry and

22    the proposal of possible processes/explanations based on distinct experimental scenarios. The

23    experiments supply information on chemical mechanisms in chalk water weakening and the

24    effect of saturation and flooding with synthetic brine solutions: $NaCl$, $Na_2SO_4$, $MgCl_2$, $CaCl_2$,

25    and seawater without magnesium (SSW-1[$Mg^{2+}$]). Two different thermodynamic conditions

26    (flooding state) were applied to the compacted cores within the creep phase: flooding steadily

27    through the core and bypassing the core, both at high temperature and high pressure. The method

28    provided measurements to investigate the effect of flow rate on the chemical reactions between

29    the rock and fluid. Yield stress level, bulk modulus value, and creep strain rate are three

30    mechanical properties of samples which were measured and analyzed together with chemical

31    analysis of effluents taken periodically during the creep phase of each experiment. The results

32    subsequently provide information about weakening/strengthening behavior within a time-

33    dependent period. Switching of flooding fluid from distilled water to the $NaCl$ solution tripled

34    the creep strain rate and produced calcium content equal to seawater concentration. Performing a

35    similar action on a distilled water to $Na_2SO_4$ solution generated enhanced creep of close to a

36    factor of three. In addition, adsorption of sulfate to the chalk surface was identified. Flooding

37    solely with $NaCl$ solution or $Na_2SO_4$ solution caused 25% and 50% decrease in chalk mechanical

38    strength compared to distilled water flooded cores, respectively. $MgCl_2$ solution flooding

39    experiments generated cores with 10% higher mechanical strength compared to cores treated

40  with $Na_2SO_4$ solution. The observation was confirmed by testing cores with SSW-1[$Mg^{2+}$] where

41  relatively low hydrostatic yield and enhanced creep strain were observed compared to $Na_2SO_4$

42  solution testing. Chalk cores flooded with $MgCl_2$ solution showed 25% and 50% lower

43  mechanical strength values compared to cores tested with NaCl and distilled water. Collected

44  samples from $MgCl_2$ and SSW-1[$Mg^{2+}$] flooding showed simultaneous processes of magnesium

45  retention inside chalk and production of calcium. Changing the flooding state to bypass with

46  $Na_2SO_4$ solution did not generate any difference in the creep strain rate whereas a change of

47  flooding state from bypass to flooding triggered production of calcium equal to one-third of

48  calcium content in seawater. However, an opposite observation was recorded when the flooding

49  state changed when using $MgCl_2$ as a flooding fluid. Change of the flooding state from flooding

50  to bypass created enhanced compaction in case of $MgCl_2$. The observed trend was similar when

51  changing from bypass to flooding in case of testing with $Na_2SO_4$ and SSW-1[$Mg^{2+}$]. The

52  extensive experiments provide a foundation for analyzing the behavior of chalk-brine in the

53  presence of oil and building verified models to simulate the effect of flooding complex brine and

54  seawater on the mechanical characteristics of chalk and predicting the chemo-mechanical

55  behavior of chalk.


56  INTRODUCTION

57  Hydrocarbon production, mining activities, and ground water removal could create a

58  downward movement of Earth's surface, compared to a reference, for example, sea-level or

59  seabed, which is addressed as subsidence. This phenomenon has received great attention in the

60  field of hydrocarbon extractions (Allen and Mayuga, 1970; Andersen et al., 1992; Dusseault,

61  1983; Fredrich et al., 1996; Ruddy et al., 1988; Schoonbeek, 1977). Reservoir compaction due to

62  hydrocarbon removal, as a consequence of surface subsidence, was detected for the first time in

63    the Goose Creek oilfield located along the Texas Gulf Coast in the U.S. (Pratt and Johnson,

64    1926). Compaction of the Ekofisk field in the Norwegian sector of the North Sea, as a costly

65    case, was recognized and reported in the late twentieth century (Smith, 1988; Sulak, 1990).

66    Researchers have attempted to explain and predict the compaction issue in the chalk layers of the

67    Ekofisk field in terms of primary depletion and rock compressibility (Andersen et al., 1992; Chin

68    et al., 1994). Although water injection in the Ekofisk field was started in 1987 in order to

69    improve oil recovery and maintain the average reservoir pressure, the subsidence is still

70    persisting (Gauer et al., 2002; Nagel, 2001; Spencer et al., 2008; Sulak, 1990). In spite of oil

71    displacement by water, the chalk immediately becomes weaker in the presence of water, a

72    phenomenon referred to as the water weakening effect of chalks. Therefore, several studies have

73    been initiated in the area of chalk-fluid interaction in order to investigate the sensitivity of chalks

74    to water from a chemo-mechanical point of view (Gutierrez et al., 2000; Heggheim et al., 2005;

75    Homand and Shao, 2000; Korsnes et al., 2008; Madland et al., 2009; Madland et al., 2008;

76    Maury et al., 1996; Risnes et al., 2003; Zangiabadi et al., 2009; Zangiabadi et al., 2011). In most

77    of these studies the effect of seawater-like brines on chalks' mechanical stability was

78    investigated. However, the presence of several different types of ions in seawater-like brines

79    makes chalk-fluid interactions complicated to analyze.

80      Experiments show molar concentration of cations in SSW is $Na^+$, $Mg^{2+}$, $Ca^{2+}$, and $K^+$,

81    mentioned in descending order. Anion components present in SSW, in descending order, are: $Cl^-$,

82    $SO_4^{2-}$, and $HCO_3^-$. The order is more or less similar in comparison to the water flooding fluid

83    components, i.e., Ekofisk brine, except the fact that sulfate is not present (Heggheim et al., 2005;

84    Zangiabadi et al., 2009). In addition, changing the salinity, total dissolved solids, in

85    waterflooding and EOR methods is not uncommon (Zangiabadi et al., 2009). Therefore, the

86    strategy in this study sets out to show how aqueous solutions of common salts (NaCl, $Na_2SO_4$,

87    $MgCl_2$, and $CaCl_2$) could affect the mechanical strength of chalk. Thereafter, the impact of more

88    complex aqueous brines, i.e., SSW-1[$Mg^{2+}$], on the mechanical stability of chalk is studied.

89    Meanwhile, answering the question on the rate dependence of fluid inside the core on the

90    mechanical behavior of the rock is attempted. Toward a comprehensive study of chalk-fluid

91    interaction, this paper combines the result of rock mechanical tests, i.e. hydrostatic loading and

92    time-dependent behavior, with chemical analysis for major ions ($Ca^{2+}$, $Mg^{2+}$, and $SO_4^{2-}$) from

93    sampled flooding effluent. Subsequently, a chemo-mechanical coupling in chalk is discussed in

94    terms of different proposed chalk-fluid weakening mechanisms such as physical and/or chemical,

95    which in turn can be used to develop a chemo-mechanical modeling of chalk in the future.

96

98      As a widely accepted observation, water-saturated chalks are mechanically weaker than dry

99      chalks. A description of this phenomena was attempted, based on the capillary forces of chalk.

100     Chalk has an open pore structure but at the same time narrow pore throats because of small

101     grains. Therefore, the capillary forces in the chalk are higher compared to the value of the

102     capillary forces in sand. Several studies were carried out with the aim of explaining chalk-water

103     interactions based on capillary forces (Andersen et al., 1992; Delage et al., 1996; Plischke, 1996;

104     Schroeder and Shao, 1996). Basically, the idea was taken from the fact that water at low

105     saturation forms capillary menisci in the small pores of chalk, which pulls the grains toward each

106     other. This attractive force is called capillary force or capillary pressure. Because of the

107     instantaneous deformation of chalk at the onset of water injection or water flooding (Newman,

108     1983), it was concluded that capillary forces, as a chalk-water interaction mechanism, are

109     responsible for the observed water weakening effect (Brignoli et al., 1994; Papamichos et al.,

110     1997). This mechanism has been questioned by Gutierrez et al. 2000 and Risnes et al. 2003).

111     They concluded that capillary effects could not solely account for the chalk-water interactions.

112     Meanwhile, some studies tend to introduce chemical effects in combination with physical

113     effects as mechanisms of interaction. Among the studies that proposed physical and/or chemical

114     mechanisms, Risnes and Flaageng (1999) suggested a possible model for the chalk-water

115     interaction that contains repulsive electrostatic and attractive (capillary) forces between chalk

116     grains. Moreover, Risnes et al. (2003) proposed water activity of the fluid in contact with chalk

117     grains as an important parameter in the field of chalk-fluid interactions. Later on, a series of

118     studies have been performed in order to scrutinize the role of chemical effects on the water

119     weakening of chalk, such as dissolution and re-precipitation, changes in surface chemistry, and

120    pressure solution. Apparently, many experiments suggest the experimental fact that chalk-water

121    interaction cannot be described thoughtfully without taking into account the role of chemical

122    effects between pore fluid and chalk (Newman, 1983; Gutierrez et al., 2000; Risnes et al., 2003;

123    Hellmann et al., 2002b; Heggheim et al., 2005; Korsnes, 2007). Therefore, the intention here is

124    to give an insight into the chemical chalk-water mechanisms relevant to the presented results,

125    rather than giving a summary of all the proposed chemical mechanisms.

126        The experimental pressure solution compaction of chalk in aqueous solutions was studied

127    comprehensively by Hellmann et al. (2002a,b). They drew a conclusion based on redistribution

128    of dissolved mass from the chalk matrix and precipitation in pore spaces. Zhang and Spiers

129    (2005) proposed that intergranular pressure solution is controlling the compaction in pure calcite

130    samples. Calcite dissolution at the grain contacts, which can cause two possible chemical effects,

131    namely local weakening and modification of calcite surface, was suggested by Gutrriez et al.

132    (2000). More recently, Korsnes (2007) suggested a chemical mechanism for water weakening of

133    chalk based on a process called "ion substitution." The suggested model was described in terms

134    of the interexchange between calcium (from the chalk surface) and magnesium (in the fluid layer

135    adjacent to the chalk surface) at intergranular contacts in presence of sulfate. The proposed

136    mechanism could lead the chalk to compact more due to incorporation of the smaller sized $Mg^{2+}$

137    ions compared to $Ca^{2+}$ ions (as part of the surface). However, the idea was challenged by a series

138    of study on rock-fluid interactions in chalk (Hiorth et al., 2008a; Hiorth et al., 2008b; Madland et

139    al., 2008; Madland et al., 2009; Zangiabadi et al., 2009; Zangiabadi et al., 2011). In these series

140    of studies, the importance of dissolution processes in chalk was stressed. Moreover, they showed

141    that $MgCl_2$ brine, which has no sulfate, causes a weakening effect in the chalk on a similar order

142    of magnitude to that of seawater as pore fluid. They also presented that calcium produces and

143  magnesium precipitates in chalk core when the chalk core flooded with brines contain no sulfate.

144  Therefore, a conclusion was drawn, yet not directly related to the weakening of the chalk matrix,

145  that dissolution and precipitation could play an important role in chalk-water interaction

146  mechanism.

147     MATERIAL, EQUIPMENT, AND PROCEDURES

148     Chalk samples and brines

149     All the tests were performed on outcrop chalk from the quarry of Stevns Klint (termed SK

150  hereafter) near Copenhagen. This chalk was used for two reasons. First, the chalk is very pure in

151  calcite content (> 98 %) (Hjuler, 2007), which simplifies analyzing the direct effects of different

152  aqueous chemistries on the mechanical behavior of chalk without concern for any other

153  perturbations. Secondly, the results obtained from this study can be critically compared with

154  previous studies as the chalk has been frequently used by other researchers (Korsnes, 2007;

155  Madland et al., 2009; Madland et al., 2010). In spite of relatively high porosity of SK chalk, 45 –

156  50 %, its permeability is usually a few mD, 2 – 5 mD, due to the fact that the pore throats are

157  rather narrow. The non-carbonate content of SK chalk (Smectite, Quartz, and Mica) is less than 1

158  %. SK chalk has a specific surface area around 2 m2/g (Hjuler, 2007). It is worth mentioning that

159  the porosities for all the prepared cores are quite similar.

160     All SK cores were saturated and tested with only aqueous solutions, synthetics brines, meaning

161  that no hydrocarbon was used during the experimental work. Therefore, SK chalk cores are not

162  oil saturated and do not have oil, and phenomena like relative permeability, oil-water

163  interactions, and others are not covered in present study. The brines were used in the study as

164  saturation and/or flooding fluid. All the brines were filtered through 0.5 μm filters after

165    preparation and degassed before usage. The brine compositions are listed in the Table 1. The

166    ionic strength of all the selected brines is equal to ionic strength of synthetic seawater of 0.657.

167

168

169    Samples preparation, equipment, and experimental procedures

170    A total of twenty-one cores were drilled with an oversized core bit, cooled by circulating

171    water. The outcrop chalks were oven-dried at about 100 ºC to constant weight (at least 24 hours)

172    before being machine-turned to the required diameter (37 or 38.1 mm). The length of cores was

173    kept at approximately 70mm (± 0.5mm) to ensure a practical rule of core length twice the core

174    diameter, accepted in experimental rock mechanics to decrease stress concentration, frictional

175    end effects, and buckling. Afterwards, the cores were saturated with distilled water (DW) using

176    an evacuator (at least three hours). Any pre-adsorbed ions in the saturated cores, for example,

177    sulfate ions, were washed out by flooding with five pore volumes (PV) of distilled water

178    (Puntervold, 2007). Finally, the cores were oven-dried and thereafter saturated with one of the

179    different artificial testing brines.

180    The triaxial cell used for rock mechanical tests in this study is a hydraulically operated cell as

181    presented schematically in Figure 1. Three high-pressure pumps control the axial pressure,

182    confining pressure, and fluid circulation. Design of the piston chamber of the cell is "auto-

183    compensated" so that the confining pressure is also applied axially. The pump in the axial circuit

184    will thus only provide an additional axial pressure, maximum seven bars, to overcome the

185    friction inside the cylindrical piston chamber and keep the piston in contact with the sample.

186    Therefore, the axial stress will always be slightly higher than the confining stress as an

187    alternative to pure hydrostatic tests in the cell. However, the loading, with good accuracy, could

188    be assumed hydrostatic. Axial deformations were measured by an outside Linear Voltage

189    Displacement Transducer (LVDT). Lateral deformation is measured by the use of a chain

190    surrounding the sample and an extensometer for measuring any difference of the circumference

191    of the cylindrical sample. The cell is equipped with a heat regulating system that allows a

192    temperature control from ambient conditions up toward 150±0.2 °C. Warming the cell up to

193    target temperature usually takes an hour to reach a stabilized temperature and is performed after

194    pressurization of confining pressure and pore pressure to 1.2 and 0.7 MPa, respectively. By using

195    vent valve and Back Pressure Regulators, the confining and pore pressure were maintained

196    constant. As shown in Figure 1, by opening the bypass valve the flooding fluid does not flow

197    through the core, hereafter in this paper referred to as "bypass condition." Closing the bypass

198    valve will re-initiate the core flood. Therefore, two different test conditions were studied in the

199    conducted experiments: (1) Continuous flooding of different brines through the core; and (2)

200    "Bypass," no flooding, by opening the bypass valve, e.g., leaving one pore volume of brine

201    inside the core. It is worth mentioning that differential pressure of 0.7MPa between the core

202    flooding inlet and outlet line was kept constant for all the tests during flooding and bypass

203    condition by using positive displacement pumps.

204    Effluent sampling was performed more or less daily during the flooding period. An auto-

205    sampler was used when several samples were sampled in rapid succession during changes in

206    flooding status or brine. Samples were collected during bypass periods. An ion chromatograph

207    (ICS-3000) measured the concentration of major cations (i.e., $Li^+$ (as a tracer), $Na^+$, $Mg^{2+}$, and

208    $Ca^{2+}$) and anions (i.e., $Cl^-$, $SO_4^{2-}$, and $SCN^-$) in the collected effluents.

209    The cores, placed in the triaxial cell, were submitted to additional flow (about 1.5 PV) prior to

210    the compression test in order to assure "perfect" saturation and equilibrium inside the core. All

211    the cores were tested mechanically (hydrostatic loading) at an elevated temperature with a pore

212    pressure of about 0.7 MPa. The test temperature in all experiments is 130 ºC, Ekofisk reservoir

213    temperature, unless otherwise stated. During the hydrostatic tests, yield stress values of the cores

214    were determined by plotting axial effective stress versus axial strain. The yield strength was

215    determined based on the method that is described in Figure 2a.

216

217        After defining the yield stress value, the samples were further loaded to approximately 2.7

218    MPa above the yield strength before they were left to creep. This approach was selected over

219    loading all cores to a constant stress level, which leads to a different post yield loading

220    timeframe, and affecting the initial state of creep stage. In addition, the primary focus after

221    loading phase is to establish a settled time-dependent behavior of chalk or in other words steady-

222    state creep stage and leaving behind any primary, transient period, or consolidation process

223    (Risnes 2001). Creep behavior is presented at two time scales: regular creep time and logarithmic

224    creep time. The slope of the creep strain-logarithmic time graph (m) is calculated and reported

225    for all the experiments, Figure 2b. In EOR operations water injector wells play a vital role.

226    However, the operation mode of injector wells are subject to periodical shut down and start up.

227    The operation mode change in real life affects the formation nearby the well, both physically and

228    chemically. The operation is simulated in these experiments by introducing two different test

229    conditions on the core: (1) Continuous flooding of different brines through the core; and (2) no

230    flooding by opening the bypass valve, e.g., leaving one pore volume of brine inside the core.

231    Both of these described conditions were applied on cores with similar brines in opposite orders.

232    First, during the loading phase and for approximately one week of creep before the test

233    conditions were changed after one week in the creep phase. The pore fluid can be assumed to be

234    in thermodynamic equilibrium with the rock sample when the core was bypassed, which means

235    no net driving force or bulk mass transfer occurs across the boundary of the system, core inside

236    the cell. The flow rate of the brine in all of the experiments is one PV/day unless otherwise

237    stated. Almost all the cores were flooded at the end of the creep phase by at least 1.5 PV of

238    distilled water.

239

240    RESULTS AND DISCUSSION

241    The results of representative stress-strain and the time dependent behavior of cores in different

242    aqueous chemistries together with a chemical analysis of effluents taken while performing tests

243    are compared and discussed in this section. The experimental results detailed here are obtained

244    using no hydrocarbon, only aqueous solutions. Therefore, topics like aging in oil, residual oil

245    saturation, relative permeability, and wettability alteration are irrelevant to the discussion in the

246    present study. However, readers interested in such topics and detailed discussions of oil

247    interaction, both mechanical and chemical in chalk cores, are invited to consult with earlier

248    authors' work (Rezaei Gomari et al., 2006; Zangiabadi et al., 2008; Zangiabadi et al., 2009).

249    A summary of results from the loading and creep phases of all experiments, only on cores

250    saturated and flooded with one individual fluid entirely, are presented in Tables 2 and 3. The

251    results are tabulated into two groups: Group 1: Core is flooded during the first week of creep

252    (first phase) before the core is bypassed in the second week (second phase); Group 2: Core is

253    bypassed during loading and the first week of creep before flooding is initiated in the second

254    week of the creep phase.

255

256    Table 2 and Figure 3a show the stress-strain behavior of all the flooded cores. The core SK2

257    treated with $Na_2SO_4$ brine tended to produce the lowest yield stress value, 4.6 MPa. This value is

258    very similar to the yield stress value obtained for the core saturated with SSW-1[$Mg^{2+}$], 4.7 MPa.

259    However, the total axial strain value within the loading phase of the $Na_2SO_4$ brine saturated core

260    is by a factor of two higher than the value recorded for the SSW-1[$Mg^{2+}$] brine saturated core.

261    The yield stress value for cores saturated with $MgCl_2$ is 5.0. The core saturated with distilled

262    water has a high yield stress value, equal to 7.7 MPa. $CaCl_2$ brine saturated cores, SK26 and

263    SK28, have an average yield stress value equal to 4.95 MPa. The stress-strain behavior of

264    bypassed cores, group 2, is illustrated in Figure 3b. The core saturated with $MgCl_2$ obtained the

265    highest yield stress, 5.7 MPa.

266

267        The yield stress value for cores saturated with $Na_2SO_4$ and SSW were close to each other, 4.8

268    and 4.85 MPa, respectively. The yield stress value of the core saturated with the SSW-1$[Mg^{2+}]$

269    brine was determined to be 4.85 MPa. All over, in the second group of Table 3, the yield stress

270    and bulk modulus values do not point toward a solid conclusion beyond themselves, yet it is

271    possible to say that all the brines that have sulfate resulted in a lower yield stress value. The core

272    saturated with SSW is the most deformed core in this group, Figure 3b. As seen from Table 3,

273    the strain rate within the bypass period for the SSW core was decreased to more than half of it in

274    the flooding period. The strain rate of cores saturated with the $Na_2SO_4$ brine and SSW-1$[Mg^{2+}]$

275    were increased to more than five times after flooding initiation.

276

277        On the other hand, obtained creep strain, Table 3. and Figure 4a, reveals that the cores

278    saturated with the $Na_2SO_4$ brine and SSW-1$[Mg^{2+}]$ were deformed the most and the core

279    saturated with the $MgCl_2$ brine obtained a lower creep strain in both phases, flooding and

280    bypassing. Additionally, these cores obtained a similar abrupt increase in the creep strain rate

281    when the flooding status was changed to bypass. It seems all brines that contain sulfate ions (i.e.

282    $Na_2SO_4$, SSW-1 $[Mg^{2+}]$) create enhanced creep strain on the cores compared to the brines

283    without sulfate ions. However, under different aqueous chemistries the yield stress and bulk

284    modulus values of cores are scattered and show no clear trend. In the following figures, Figure

285    4a and Figure 4b, the time dependent behavior of the cores either flooded or bypassed is

286    illustrated. Core SK3, saturated with distilled water, obtained the least axial creep strain, owning

287    the value of 0.15 %, Table 3. Axial creep strain for the core saturated with $MgCl_2$ started to

288    increase after the onset of the bypassing period, as shown in from Figure 4a. The core saturated

289    with the $Na_2SO_4$ brine and the core saturated with SSW-1[$Mg^{2+}$] showed quite similar creep

290    behavior, Figure 4b. The core saturated with NaCl brine deformed less than the $Na_2SO_4$ and

291    SSW-1[$Mg^{2+}$] brine saturated cores, but obtained more axial creep strain compared to the $MgCl_2$

292    brine saturated core. All the cores that were flooded after one week of creep are presented in

293    Figure 4b. In this case, the core saturated with SSW deformed the most, followed by the core

294    saturated with the $Na_2SO_4$ brine. The axial creep strain curves overlap for the core saturated with

295    $MgCl_2$ and SSW-1[$Mg^{2+}$] until the onset of flooding. SSW-1[$Mg^{2+}$] flooding tended to deform

296    the core more within the flooding period, compared to the $MgCl_2$ brine.

297

298    Chalk-water Interaction in the Absence of Ions (reference case)

299    In order to get a better understanding and documentation of the influence of different aqueous

300    chemistries on the mechanical strength of the chalk, mechanical tests on a core saturated with

301    distilled water were conducted as reference experiment. Core SK3 was saturated with distilled

302    water and hydrostatically tested, obtaining a yield stress value of 7.7 MPa, Table. 2. Therefore,

303    the hydrostatic loading increment was stopped at 10.5 MPa. Total axial strain within the loading

304    phase was around 0.80 %. The core obtained just 0.15 % total axial creep strain after three days

305    of creep with flooding (4589 minutes), Figure 5. The slope of creep strain versus the time within

306    the creep stage is calculated to be 0.06 %/time decade, Table 3., SK3.

307

308      Saline Solution Flooding

309    In this section, the impact of saline solutions, NaCl and $Na_2SO_4$ brines, on the mechanical

310    stability of the chalk cores, saturated and flooded with distilled water from the beginning of the

311    loading phase until a certain time during creep period, is demonstrated. Therefore the cores'

312    properties are listed separately, Table 4. It is worth mentioning that 0.2 MPa difference in yield

313    stress value, subsequently creep stress value) will not result in increase of strain rate by factor of

314    two. However, it should be noted that the methodology and experimental procedure is the same

315    as described in samples preparation, equipment, and experimental procedures section.


316    Solutions of NaCl were addressed as indifferent brine toward chalk according to studies

317    performed by Pierre, 1990; Rezaei Gomari et al., 2006; and Strand et al., 2006. In order to verify

318    the effect of NaCl flooding on the compaction behavior of chalk, a compression test was

319    designed on a core pre-saturated by distilled water, core SK20. The core was loaded up to 9.3

320    MPa, 2.8 MPa higher than its yield stress value (6.5 MPa).

321    The duration of the creep stage of core SK20, flooded with distilled water, was almost four

322    days. Subsequently, the flooding fluid was switched to the NaCl brine which clearly had an

323    impact on the creep strain rate, Figure 6. Introducing the NaCl brine increased the compaction

324    rate of the core by a factor of three, from 0.08 %/day to 0.25 %/day. However, after flooding 15

325    PV of NaCl brine, the compaction rate was slightly lower than the compaction rate at the end of

326    the period of distilled water flooding, 0.05 %/day.

327    In order to measure any possible adsorption of $Na^+$ ion on to the chalk surface 1.02 g LiCl

328    tracer in 1 liter of NaCl brine solution, Table 1, was introduced to the core SK20 during the creep

329    stage, as the flood was performed. The ion chromatograph (ICS-3000) measured the

330    concentration of three major cations, $Li^+$, $Na^+$, and $Ca^{2+}$, by analyzing some of the water samples

331    collected at the core outlet. The relative concentration of $Na^+$ and $Li^+$ is plotted versus pore

332    volume of the injected brine, Figure 7a. The small area between the relative concentration of $Na^+$

333    and $Li^+$ ions, adsorption curves, illustrates that only negligible amounts of $Na^+$ ions have been

334    adsorbed in the core. Additionally, the concentration of calcium was plotted in Figure 7b.

335    Concentration of $Ca^{2+}$ ions in SSW was used as calcium reference concentration due to the fact

336    that no calcium is presented in the NaCl brine. It is shown that the concentration of calcium was

337    increased to calcium reference concentration when one pore volume of NaCl brine was flooded

338    through the core. Eventually, calcium concentration is decreased and stabilized around 30 % of

339    calcium reference concentration.

340    Another rock mechanical test was conducted on core SK5A, initially saturated and flooded

341    with distilled water. The aim was to perform an adsorption test of sulfate onto the grain surfaces

342    before and after the hydrostatic loading. Therefore, the core-flood of distilled water was first

343    switched to 2.33 gram of KSCN in 0.219 M $Na_2SO_4$ brine. The relative concentration of these

344    ions, compared to the original brine, versus pore volume of flooded brine is illustrated in Figure

345    8a. It can be noticed that the dispersion front of SCN- corresponded to about 0.5 PV.

346    Additionally, the tracer curve passed the point, (PV, C/C0) = (1, 0.5), which means that the

347    injected fluid is in contact with the total pore volume of the core. The breakthrough curve of

348    sulfate ion was moved toward higher flooded pore volumes due to adsorption of sulfate ions.

349    Finally, the total area between the two adsorption curves is calculated, using a trapezoid method,

350    to be 0.26.

351    After performing the adsorption test, the core was cleaned by flooding several pore volumes of

352    distilled water. Distilled water flooding was continued until no sulfate was detected by a

353    qualitative batch test. Thereafter, the core was hydrostatically loaded to 8.2 MPa, creep stress

354    level. The creep period is shown in Figure 8b. The flooding fluid was switched to the $Na_2SO_4$

355    brine after 4745 min (around three days, Figure 8b) while the effluents were taken periodically,

356    Figure 8a. Obviously, the brine had a dramatic effect on the axial creep rate. The axial creep rate

357    is increased from 0.5 %/time decade during the period of distilled water flooding to a three times

358    higher value, 2.41 %/ time decade, by introducing the $Na_2SO_4$ brine, Table 4. The

359    chromatographic separation between $SCN^-$ and $SO_4^{2-}$ was tested for this compacted core, core

360    5A, within the creep phase, Figure 8a. The area between the effluent curves of the two

361    components was slightly changed, 0.25. Notably, the breakthrough for both tracer and sulfate

362    happened a little sooner in the compacted core.

363    Role of Sodium in NaCl Brine-Chalk

364    A hydrostatic compression test followed by two weeks of creep phase was performed on core

365    SK8, which was saturated with the NaCl brine. The core was loaded up to 9.4 MPa of isotropic

366    differential stress during the hydrostatic compression period, Table 2. The yield stress point and

367    bulk modulus were determined to be 6.2 MPa and 0.5 GPa, respectively. The axial strain of this

368    core at the end of the loading phase was measured to be 1.33 %.

369    During the following creep phase (Figures 9a and b), a sudden deviation occurred after

370    approximately 5500 minutes (about four days) where the pore pressure was partly lost for a short

371    period. However, the impact was not major and the trend showed a normal gradual rise before

372    the flooding was shut off at 9973 minutes, Figure 9a. This can also be seen from Figure 9b where

373    a flat trend was observed before the status of flooding was changed. The slope of axial creep

374    strain was approximately 0.45 %/time decade and is not influenced when the flooding status was

375    changed to bypass, Table 4 and Figure 9.

376  Chalk cores saturated with distilled water have been shown to be the strongest core from the

377  mechanical point of view among all the fully water saturated cores (Risnes, 2001; Risnes et al.,

378  2003; Madaland et al., 2008). The result of distilled water saturated core, SK3, is an indication

379  for the above statement since the hydrostatic yield stress value for this core was found to be 7.7

380  MPa, the highest value among all the obtained values for yield stress listed in Table. 2.

381  Additionally, the total axial strain value, obtained within the loading phase, is less than 1 %

382  which is the least value, comparing to the axial strain value for all the other brine saturated cores.

383  In parallel with the loading results, looking at the creep behavior of this core, SK3, showed that

384  the core was deformed only 0.15 % under 10.5 MPa creep stress level after three days of creep,

385  Figure 6 and Table 3.

386  The mechanism of chalk compaction, which was documented in terms of displacement, could

387  be manifested as spatial translation and rotation of calcite grains without significant collision,

388  and subsequently the breaking up of the grains called cataclasis process (progressive fracturing

389  and comminution of rock) (Powell et al., 1994). Many researchers have investigated chalk/water

390  interaction and discussed the various mechanisms in terms of physical and/or chemical effects

391  (Andersen et al., 1992; De Gennaro et al., 2003; Gutierrez et al., 2000; Heggheim et al., 2005;

392  Korsnes, 2007; Papamichos et al., 1997; Risnes et al., 2003; Schroeder and Shao, 1996). One or

393  a combination of the above mentioned chalk/water interactions, depending on the type of pore

394  fluid, might assist or enhance chalk compaction mechanism. It is worthwhile to mention that

395  saturation of dry chalk with different pore fluid caused a weakening effect on the mechanical

396  strength of chalk in the following order: dry < oil < methanol < water. The dry chalk showed the

397  highest yield stress value, followed by chalks treated with oil and methanol, respectively. The

398  chalk saturated with water possess the weakest mechanical strength.

399    According to the above explanation, the enhanced weakening effect of distilled water as

400    observed in core SK3 could be explained both physically and/or chemically. The physical

401    mechanism, capillary phenomena, was adopted from soil mechanics in partially saturated porous

402    media (mechanisms of chalk water interactions). Water injection into chalk within compression

403    tests on chalk resulted in an instantaneous compaction, which was discussed in terms of capillary

404    forces (Brignoli et al., 1994; Schroeder and Shao, 1996). It was proposed that water flooding

405    could destroy water bridges in dry or partially saturated chalks. In other words, full water

406    saturation could diminish the cohesion of material and subsequently the mechanical strength of

407    chalk. However, findings after more investigation downgraded the role of capillary forces in

408    water weakening (Risnes, 2001; Risnes et al., 2003). Chemical mechanisms have been paid more

409    attention in a series of investigations (Gutierrez et al., 2000; Korsnes, 2007; Risnes et al., 2003).

410    Distilled water could affect the surface property of chalk or facilitate the dissolution of chalk

411    (Gutierrez et al., 2000; Pierre et al., 1990). Measurement of zeta potential shows the change of

412    surface charges for chalk powders treated with distilled water and synthetic brines (Kolnes et al.,

413    2008).

414    Although the solubility of calcite in distilled water is not high (Segnit et al., 1962), distilled

415    water could cause the easier abrasion and dissolution of asperities at intergranular contacts, thus

416    assisting the sliding and rotation of the grains. The local process resulted in a weakening process

417    in the case of a distilled water saturated core in comparison with the dry core. Finally, it should

418    be emphasized that, yet again, distilled water caused less weakening to the chalk core when

419    compared to all the other aqueous solutions, e.g., different brines.

420    The NaCl solution was shown as an indifferent fluid toward calcite/chalk surface (Pierre et al.,

421    1990; Rezaei Gomari et al., 2006). However, our experiments clearly showed an actual effect of

422   fluid substitution from distilled water to the NaCl brine within the creep phase, Figure 6. It is

423   presented in Figure 7a that the adsorption of $Na^+$ ions towards calcite is negligible, while

424   introducing NaCl resulted in calcium production, Figure 7b. Thus, the observed weakening in

425   chalk strength is not due to adsorption of sodium ions to the surface but is likely a result of the

426   dissolution of chalk in the NaCl brine. Newman (1983) showed that subjecting the chalks to non-

427   equilibrated waters induces dissolution and, subsequently, mechanical instability. Moreover,

428   Millero et al. (1984) measured the solubility of calcite in solutions of NaCl at 25 ºC. In their

429   experiments, the concentration of $Ca^{2+}$ did not exceed 0.006 mol/l. An atomic force microscopy

430   of calcite dissolution in saline solutions showed that the dissolution rate of calcite increased in

431   concentrated NaCl (Ruiz-Agudo et al., 2009). It was shown that salinity, i.e., NaCl content, plays

432   a very significant role in the solubility of calcite and the kinetics of calcite dissolution and

433   precipitation (Mucci, 1983). The solubility of calcite in saline solutions was increased at

434   temperatures up to 300 ºC (Ellis, 1963). In a study by Zhang and Spiers (2005), the compaction

435   strain rates of calcite samples in 0.1 - 0.5 M NaCl brine and salinity-free samples were compared

436   to each other. The saline samples were compacted three times more than the salinity-free

437   samples. In light of the above experimental facts, it appears that salinity is the key parameter in

438   the observed behavior of NaCl flooding on the compaction strain rate of chalk, Figures 6 and 7.

439     Core SK8 was initially saturated with a 0.657 M NaCl brine. The hydrostatic yield stress value

440   is the second lowest value, compared to all the other experiments, Table 2. Furthermore, in the

441   experiment on core SK8, NaCl brine, the flooding status was changed to bypass in order to

442   quantify the impact of the shut-in period. The aim of the shut-in period within the creep phase of

443   the rock mechanical experiments is to evaluate diffusion, kinetics, and transport processes in the

444   chalk/fluid system. The creep strain and rate of deformation has not been influenced by inserting

445     any changes in the fluid flow path, Figures 9a and b. The diffusion of $Na^+$ ions in the core, within

446     the bypass period, has not shown any impact on the creep behavior of the core. Also it has been

447     shown that shut-in and reinjection of NaCl did not affect the compaction behavior of the core.

448     However, introducing the NaCl brine to a clean core increased the compaction rate, Figure 6.

449     Based on the observation from Figure 7b, it could be considered that the NaCl brine increased

450     the dissolution of the chalk; hence, it enhanced the compaction of the core within the time

451     dependent period.

452     Role of Sulfate in $Na_2SO_4$ Solution Flooding

453     One core, SK5A, was saturated and flooded with distilled water within the first three days of

454     creep stage; thereafter, $Na_2SO_4$ brine was introduced to the system containing chalk and distilled

455     water, Figure 8b. In this section, the results of the rock mechanical tests, both from hydrostatic

456     compression and creep phase, on cores saturated with $Na_2SO_4$, are presented. Core SK2,

457     saturated with $Na_2SO_4$, was hydrostatically loaded to 7.7 MPa of differential stress since the

458     yield stress value was defined as 4.6 MPa, Table 2. Total axial strain obtained within the loading

459     phase was around 2.2 % and the bulk modulus for this core was determined to be 0.32 GPa.

460     The core was flooded for 9683 minutes (about a week) before changing the flooding status to

461     bypass, Figure 10a. The flooding status was changed when the creep strain had reached a steady

462     trend, Figure 10b. The illustration in Figure 10b shows that the deformation rate was

463     approximately 1.21 %/time decade in this period and it did not change after shutting off the flow

464     of pore fluid in the core, Table 3. At the end of the test, flooding of distilled water did not cause

465     any additional effect on the slope of creep curve. The value of yield stress, core SK2, is smaller

466     than the value for cores saturated with distilled water and NaCl brine, comparing values in Table

467     2. The comparison is in line with rock mechanical experiments performed on the other chalk

468     outcrops (Madland et al., 2009). The zeta potential measurement of the suspension of chalk

469     powder/ $Na_2SO_4$ brine showed that sulfate ions can change the surface potential of the chalk

470     towards negative values by forming an adsorption layer around chalk grains (Kolnes et al., 2008;

471     Rezaei Gomari et al., 2006). Therefore, it is concluded that sulfate ions could adsorb to the chalk

472     surface through a thin layer adjacent to the chalk grains; consequently, the potential of the

473     surface could be changed toward negatives values. The electrostatic force created by this layer,

474     as a repulsive force between grains, could be responsible for the observed weakening behavior

475     under the influence of sulfate-rich brines (Risnes and Flaageng, 1999; Hiorth et al., 2008a;

476     Hiorth et al., 2008b; Madland et al., 2009). The switch from flooding to bypass did not generate

477     any deviation in the steady state time dependent behavior of core SK2, as depicted in Figure 10a,

478     b. Therefore, the diffusion of $SO_4^{2-}$ ions, if any, does not affect the compaction rate of the core

479     fully saturated with the $Na_2SO_4$ brine.

480       It is shown that the concentration of $Na^+$ and $SO_4^{2-}$ ions in the sampled effluents was more or

481     less around the original concentration of these ions in the $Na_2SO_4$ brine, Figure 11a. Chemical

482     analysis of the sampled effluent at the core outlet, core SK2, shows that in comparison with the

483     concentration of calcium in seawater, only a little calcium is produced during the flooding

484     period, Figure 11b. The calcium concentration remains stable within the bypass period which is

485     expected since the flooding brine contains no calcium. When distilled water was flooded through

486     the core, the production of calcium increased and reached the amount of one-third of the

487     seawater concentration in the last three collected samples.

488

489     Core SK5 and SK6, saturated with 0.219 M $Na_2SO_4$, were also mechanically tested, but in this

490     case the brine was bypassing the cores for one week of creep. These cores were loaded to 7.6

491    MPa and 7.7 MPa of isotropic differential stress since the point of yield stress for cores SK5 and

492    SK6 was found out to be 4.8 MPa and 5.9 MPa, respectively. Since the result of hydrostatic

493    loading on core SK5 was reproduced in the experiment on the core SK6, only the bulk modulus

494    value and total axial strain of core SK5 is shown in Table 2.

495    The flooding status was changed from bypass to flooding after about a week for both cores

496    (9584 minutes for core SK5 and 9567 minutes for core SK6), as seen in Figure 12a. From Figure

497    12b, a change in the slope of creep strain becomes obvious when the cores are bypassed

498    compared to the flooding period. The axial creep strain rate, valid for both cores SK5 and SK6

499    during the bypass period, is 0.5 %/time decade, which is increased to 2.9 %/time decade within

500    the flooding period, Table 3. The flow rate of the brine through core SK6 was increased to 2

501    PV/day after two weeks of creep (20703 minutes) which did not tend to create any deviation on

502    the slope of the creep curve, Figure 12a. Distilled water flooding also had no impact on the creep

503    trend. The rock mechanical test on core SK5 was performed in the same manner as in the test on

504    core SK6. After a similar creep trend was obtained, the flooding brine was changed from $Na_2SO_4$

505    to SSW-1[$Mg^{2+}$] at around 12834 minutes (about 9 days), Figure 12a. The brine was substituted

506    during the steady state of the creep phase. The intention for this change was to study the effect of

507    $SO_4^{2-}$ ions on the chalk in the presence of calcium. Core SK5 was predicted to follow the same

508    trend as core SK6 if the brine had not been changed and any diversion from the predicted trend is

509    therefore assumed to be caused by the new brine. Apparently, no change was observed due to

510    this substitution. The core was flooded by distilled water at the end of the creep phase which had

511    no impact on the creep behavior.

512    In the experiments conducted on cores SK5 and SK6, the objective is to examine the influence

513    of flooding initiation of the $Na_2SO_4$ brine to the cores, which are entirely bypassed from the

514     beginning of the loading phase and the first week of the creep phase, Figures 12a and b. First, the

515     result of hydrostatic loading, listed in Table 2, indicates that the average yield stress value of

516     cores SK5 and SK6 is very close to the value for core SK2, treated with $Na_2SO_4$. In addition, the

517     mean bulk modulus value for cores SK5 and SK6 is reasonably similar to the calculated value for

518     core SK2, treated with $Na_2SO_4$. A substantial difference appeared during the creep phase of core

519     SK5 and SK6 in comparison to the creep behavior of core SK2, Figures 11a and 13a. When the

520     bypass period changed to flooding after one week of creep, a substantial deviation happened in

521     the slope of the axial strain. This clearly shows the effect of flooding fresh $SO_4^{2-}$ ions and,

522     consequently, disturbing the equilibrium condition inside the core. The brine, an $Na_2SO_4$

523     solution, has a concentration of sulfate ions ten times higher than the concentration of sulfate in

524     SSW. However, the solution has an ionic strength similar to NaCl brine; hence, the observed

525     enhancement on the axial creep strain could not be explained by the difference in the ionic

526     strength.

527      In Figures 14a and b the chemical analyses of the effluents that were taken during the bypass

528     and flooding periods of the test on core SK6 are plotted. The status change from bypass to

529     flooding had no effect on the concentration of sodium and sulfate, Figure 13a. The concentration

530     of calcium was increased after the change in the flooding status, Figure 13b.

531

532      A possible explanation would be the abrasion and dissolution of chalk grains (Hiorth et al.,

533     2008a, b). Some studies showed that $SO_4^{2-}$ ions have the ability to make an ion pair with the

534     desolvated ions from the surface of calcite and lead to enhanced dissolution (Ruiz-Agudo et al.,

535     2009). The thickness of the adsorbed layer of sulfate ions onto the chalk surface is on the order

536     of the molecular diameter that is surrounded by the hydrodynamic boundary layer and bulk

537    solution. The thermodynamic equilibrium in the aquatic system, saturated chalk and solute, could

538    be disturbed by flooding initiation, characterized by the flow of sulfate ions in the bulk solution

539    and affecting the already formed adsorption layer around the chalk grains. As a principle, any

540    change in the equilibrium condition of a system would cause the system to counteract the effect

541    of the change. If the concentration of sulfate ions inside the bulk solution is assumed to be

542    increased markedly, over a short period of time after flooding, some counter-ions, cations such

543    as $Ca^{2+}$, need to be added in order to turn back the system to the equilibrium condition. The

544    deficit of counter-ions in the bulk solution should be supplied by a dissolution of $Ca^{2+}$ from the

545    chalk grains. Based on this scenario, the amount of calcium ions in the effluents was increased.

546    As shown in Figure 13a, the concentration of sulfate as well as the sodium ions concentration

547    remained stable after initiation of the flooding phase for one week of creep. Figure 13b shows

548    that calcium is also produced around 30 % of calcium reference concentration when the flooding

549    is started. The observed weakening effect could be explained, yet not directly, by dissolution

550    from calcite grains.

551    Role of Magnesium in the Brine-Chalk System

552    Core SK7 was saturated with 0.219 M $MgCl_2$ brine. The applied hydrostatic stress was

553    increased to 9.2 MPa, creep stress level, and kept constant. The yield stress value was

554    determined as 5.7 MPa, Table 2. The values of bulk modulus and total axial strain of the core

555    SK7 are reported in Table 2 as 0.46 GPa and 1.82 %, respectively.

556    The core was bypassed during the first six days of creep, Figure 14a. The obtained axial strain

557    was 1.27 % and the core deformed with the rate of 0.84 %/time decade, Figure 14b and Table 3.

558    The first change from bypass to flooding was made after 8550 minutes. The core flood was

559    continued for one week and a decrease in the deformation rate was detected, 0.37 %/time decade,

560    Table 3. It is also clear from Figure 14a that the creep trend immediately shows a flattening

561    creep. Thereafter, by bypassing the core, the creep rate was increased again, 0.77 %/time decade,

562    Figures 14a, b. The final change, where the status was changed back to flooding, was done after

563    23378 minutes (about 16 days). The flooding rate was increased to 2 PV/day during this period

564    and the deformation rate did not change substantially compared to the pervious flooding phase. It

565    is obvious from Figure 14a that within flooding periods the rate of deformation was slowed

566    down.

567

568    Additional tests, involving cores flooded with 0.219 M or 0.110 M $MgCl_2$ brine within the

569    loading phase and the first week of creep, were conducted in order to elaborate the observed

570    behavior of core SK7 during the bypass period, Figures. 14a, b. In a creep test performed on core

571    SK1, illustrated in Figure 15a, it was observed that the deformation rate was increased after the

572    flow of brine into the core was shut off. Apparently, the obtained creep strain was increased from

573    0.85 % to 1.3 % after one week of bypass. Additionally, the creep strain rate was increased from

574    0.3 %/time decade within the flooding phase to 1.7 %/time decade during the bypass period,

575    Figure 14b.

576    The observed phenomenon was confirmed in other tests using a lower concentration of $MgCl_2$

577    brine, 0.110 M, as saturation brine, Figures 15a, b. The figures also show that the cores saturated

578    with a lower concentration of $MgCl_2$ brines, core SK22 and SK25, obtained more creep during

579    the bypass period. It is worth noting that the creep strain of these cores is in comparison with the

580    core saturated with a higher concentration of $MgCl_2$ brine, 0.219 M, core SK1.

581

582    Rock mechanical experiments on cores saturated with $MgCl_2$ brine showed that bypassing with

583    $MgCl_2$ during the shut-in period causes an enhancement in the deformation rate within the creep

584    phase, Figures 14 and 15. Additionally, saturation of the cores with a half concentration of

585    $MgCl_2$ brine, 0.110 M, and bypassing them also caused an enhancement in the obtained value for

586    the axial creep strain, Figures 15a and b; however, to a lesser extent.

587    To attain a better understanding of the chemical reactions between the $MgCl_2$ solution and

588    chalk, the concentration of major ions ($Mg^{2+}$ and $Ca^{2+}$) in the effluents, taken periodically during

589    the creep phase at the outlet of core SK7, was measured by the ion chromatograph. The

590    concentrations of $Mg^{2+}$ and $Ca^{2+}$ ions in the effluents are plotted in Figure 16. In the figure the

591    original concentration of magnesium (0.219 M) and the calcium concentration in SSW (0.013 M)

592    are included as reference values. The x-axis in Figure 16 corresponds to the x-axis in Figure 14a.

593    During the first phase, bypass, the concentration of $Mg^{2+}$ is fluctuating around its original

594    value and no calcium is detected. Flooding with the $MgCl_2$ brine causes a sudden drop in the

595    magnesium concentration; whereas, it increases the calcium concentration. After its initial

596    maximum, the $Ca^{2+}$ concentration during the flooding phase, the concentration of calcium is

597    finally close to concentration in seawater, 0.013 M. No sampled effluents were analyzed from

598    the second bypass period. As soon as the core flood is initiated again, the concentrations of

599    magnesium and calcium follow the imaginary extrapolation of the trend within the flooding

600    period. At the end of the experiment, the calcium concentration decreased and stabilized a little

601    below the concentration in seawater; the concentration of magnesium is close to the original

602    $Mg^{2+}$ ion concentration. A clear observation could be drawn as magnesium is retained inside the

603    core and calcium is being produced during the flooding phases.

604

605    It was stated that within the bypass period, diffusion and transport phenomena are of great

606    importance. It is indicated in Figure 16 that an intricate chemical chalk/fluid interaction occurred

607    due to the $MgCl_2$ brine as saturation brine. Within the flooding periods, magnesium is retained

608    inside the core; meanwhile, calcium is produced. Initiation of flooding, after the first bypass

609    phase, contributed to a dramatic decrease in the magnesium ions concentration and substantial

610    production of calcium ions. As the experiment progressed with time, concentration of

611    magnesium ions is recovered sharply toward the magnesium reference concentration, 0.219 M.

612    Concurrently, calcium production is stabilized around 0.013 M, calcium reference value, after a

613    gradual decline. Retention of magnesium and production of calcium during the experiment

614    clearly indicated the existence of the two opposing reactions: dissolution (calcium production)

615    and precipitation (magnesium-bearing minerals). A series of similar experiments showed that

616    $MgCl_2$ brine has a significant weakening effect on the mechanical strength of Liège chalk

617    (Madland et al., 2009). The observed weakening effect could be discussed in terms of

618    precipitation of magnesium bearing minerals and dissolution of calcium from the chalk. The

619    proposed explanation is not directly linked to the weakening of the chalk matrix. However, the

620    dissolution and precipitation, together with any possible change in the surface charge could be

621    the dominant factors in the weakening mechanism of chalk (Zangiabadi et al., 2009).

622    In this study, the enhanced deformation of the $MgCl_2$ brine saturated cores within the bypass

623    period could be explained tentatively by the following hypothesis. During the flooding phases,

624    $MgCl_2$ brine has a tendency to flow through the highly permeable zones (macro-porosity pores)

625    of the porous medium (chalk). Diffusion to the low permeable zones and transport-controlled or

626    surface-controlled dissolution and precipitation of solute are the dominant phenomena as soon as

627    flooding has been stopped. These types of reactions, dissolution and precipitation, in low

628    permeable zones (nano-porosity pores) which assist the compaction of the chalk, sliding, and

629    rotation of grains, might explain the observed enhanced weakening. The sketch in Figure 17

630    explains the flow paths within the flooding phase and probable pathways within the bypass

631    period.

632

633    CaCl$_2$ Solution Flooding of Chalk Cores

634    Two cores, saturated and flooded continuously with 0.219 M CaCl$_2$, were tested mechanically.

635    The hydrostatic loading and creep behaviors of these cores are presented in Figures 18a and b.

636    The average value of yield stress for cores SK26 and SK28 is 4.95 MPa. The hydrostatic phase

637    of these two cores was almost identical, which can be seen from the values reported in Table 2.

638    The cores were left to creep under 6.6 MPa isotropic differential stresses, Figure 18a. The

639    average deformation of the cores reached 0.93 % after a week (about 10000 minutes) and the

640    strain rate was 0.45 %/time decade. The Ca$^{2+}$ concentration in the sampled effluents, taken

641    during the creep phase of the test on core SK26, was determined by ion chromatography, Figure

642    18b. The Ca$^{2+}$ concentrations do not show a clear trend during the creep phase/sampling period;

643    they vary around the original Ca$^{2+}$ concentration (0.219 M) in the brine.

644

645    The amount of dissolved calcium carbonate in the brine, 32.2 g/l, roughly corresponds to the

646    concentration of this salt in typical formation brines, e.g., Ekofisk brine. Moreover, activity of

647    the equilibrium chalk powder with CaCl$_2$ brine is around 0.99, according to the fluid properties

648    taken from a table inHughes, 1999. In a study by Risnes et al. (2003), the rock mechanical test on

649    cores saturated with NaCl and CaCl$_2$ brine, showed that the mechanical stability can be described

650     independent of the type of ions presented in the pore fluid. Thus, it concluded that the water

651     activity plays an important role in the weakening process of chalk.

652     In the present experiments, the ionic strength of NaCl and $CaCl_2$ brine are similar, Table 1.

653     Apparently, adsorption and/or precipitation from $CaCl_2$ brine would not be the case in the

654     condition of our study. Similar values of the axial creep deformation are obtained for the cores

655     saturated with NaCl and $CaCl_2$, Figures 18a and b. Therefore, the observed similar compaction

656     could be explained by the salinity of the brines.

657     Verification Tests: Flooding of Seawater Without Magnesium ($SSW-1[Mg^{2+}]$)

658     Cores SK4, SK16, and SK11 were saturated with SSW without magnesium ($SSW-1[Mg^{2+}]$).

659     Hydrostatic compression tests were conducted on all of these cores, Table 2. Core SK16 was

660     flooded from the beginning of the loading phase to the end of the first week of creep stage

661     whereas the brine bypassed core SK4 and core SK11 in the same period. The yield stress value

662     for cores SK4, SK16, and SK11 was found to be 5.7, 4.7, and 4 MPa, respectively. Accordingly,

663     the creep stress level was set to 9, 7.9, and 6.9 MPa. The average axial strain by the end of the

664     loading phase for cores SK4 and SK11 is very similar to the value for SK16, Table 2. Both cores

665     SK4 and SK11 deformed less within the first week of creep stage compared to core SK16, Figure

666     19a. At the end of the first week of creep, the total axial creep strain of core SK16 is close to 2

667     %, around two times higher than the axial creep strain of cores SK4 and SK11 at the same time.

668     As soon as the flooding is initiated, the axial creep deformation of cores SK4 and SK11 begins to

669     increase. In core SK16, the same behavior can be seen when flooding is again initiated (at around

670     26000 min creep time), after a period of bypass for ten days.

671     The axial creep strain for core SK11 is changed from 0.46 %/time decade within the bypass

672     period to 2.3 %/time decade after initiation of flooding, Figure 19b and Table 3. On the other

673     hand, the axial creep strain for core SK16 remains stable around 1.43 %/time decade until the

674     second stage of flooding, Figure 19b. The axial creep strain of cores SK16 and SK4 are on top of

675     each other from 26000 minutes. After three weeks of creep (21500 min), the flooding rate was

676     decreased for core SK11 to one half of its original value. The drop in the flow rate had no effect

677     on the axial creep strain rate.

678

679     In a study by Korsnes (2007), it is shown that seawater without magnesium, at a temperature of

680     90 ºC, could cause more axial strain within the creep phase compared with the seawater. It was

681     suggested that an irreversible thermodynamic condition could be responsible for the observed

682     behavior. Additionally, in a study by Madland et al. (2008) on a different type of chalk, the cores

683     saturated with seawater without magnesium obtained more deformation during the creep stage

684     than the cores saturated with seawater. This observation was also seen in experiments performed

685     by Zangiabadi et al. (2009 and 2011). They showed that SSW-1[$Mg^{2+}$] could facilitate the

686     formation of anhydrite and promote increased CaCO3 dissolution due to the reduced

687     concentration of $Ca^{2+}$ ions in the equilibrium solution. Further, it was concluded that for both

688     higher and lower porosity chalks, the impact of varying the flooding fluid causes a weakening in

689     the following order: distilled water < seawater without sulfate < seawater < seawater without

690     magnesium.

691     The behavior of cores saturated with SSW-1[$Mg^{2+}$] brine within the loading phase can be seen

692     in Figures 3a and b, which shows that the cores have quite a low yield point, most likely due to

693     the presence of sulfate ions. Heterogeneity of the chalk could explain the scatter in the yield

694     strength and obtained strain within the loading phase (Korsnes, 2007). Time dependent behavior

695     of these cores is illustrated in Figures 18a and b. Sulfate ions in the brine, SSW-1[$Mg^{2+}$], could

696    be responsible for some aspects observed in the creep stage of the cores (role of sulfate in

697    $Na_2SO_4$ solution flooding). Thus, the results were explained by the use of similarities found in

698    the experiments on the cores saturated with $Na_2SO_4$ brine. Apparently, the higher value of the

699    axial creep strain within the flooding period compared to the bypass phase, both during the first

700    creep phase, is similar to the behavior of the cores saturated with the $Na_2SO_4$ brine. Thus, the

701    weakening effect is more pronounced when the brine is flowing through the pores.

702      One can see that initiation of flooding after one week of bypass caused the axial creep strain to

703    increase, Figure 19 and Table 3. The observed impact is similar to what happened after flooding

704    the $Na_2SO_4$ brine to the bypass core, Figures 12a and b. Due to the close correspondence of the

705    two creep phases, sulfate ions could be assumed to be responsible for the pronounced axial creep

706    deformation after the initiation of flooding SSW-1[$Mg^{2+}$]. It was stated that sulfate ions could

707    firmly adsorb to the chalk surface (role of sulfate in $Na_2SO_4$ solution flooding). The statement is

708    based on the surface potential measurement of chalk powder that was not disturbed when the

709    flooding state switched to bypass (diffusion). However, when changing from bypass to flooding,

710    the bulk flow of new sulfate ions could easily disturb the equilibrated system, chalk-pore fluid,

711    and initiate an irreversible, e.g., dissolution, reaction inside the core. The phenomena could be

712    explained by the ability of sulfate ions to make an ion pair with available desolvated calcite

713    surface ions. This formation of an ion pair is disrupted by the initiation of flooding, thus causing

714    enhanced weakening. On the other hand, the changing flooding status has a reverse effect on

715    weakening, when the brine is $MgCl_2$. The diffusion and transport phenomena are playing a

716    critical role when the $MgCl_2$ brine is not flooded through the core where retained magnesium

717    from the flooding phase initiated the calcium production process.

718      CONCLUDING REMARKS

719    A systematic approach was encountered to investigate the rock mechanical behavior of chalk

720    reservoirs in presence of variety of water compositions. The aqueous solutions of common salts

721    (NaCl, $Na_2SO_4$, $MgCl_2$, and $CaCl_2$) as well as a more complex aqueous brines, i.e., seawater

722    without magnesium (SSW-1[$Mg^{2+}$]), were selected to examine their effects on the mechanical

723    strength of chalk. Additionally, two different test conditions were studied in the conducted

724    experiments: (1) Continuous flooding of mentioned brines through the core under test; and (2)

725    No flooding by opening the bypass valve; leaving one pore volume of brine inside the core. The

726    results were discussed in terms of hydrostatic loading and time-dependent behavior, with

727    chemical analysis for major ions ($Ca^{2+}$, $Mg^{2+}$, and $SO_4^{2-}$) from sampled flooding effluent. The

728    conclusions of the work are briefly listed as follows:

729

730    •    Certain types of mechanisms could explain the chalk/fluid interaction in the presence of

731    individual ions

732    •    Salinity is the key element when it comes to chalk water weakening

733    •    Seawater without magnesium and $Na_2SO_4$ brine could substantially weaken the chalk

734    •    Creep strain and its rate was found out to be similar for cores saturated with $MgCl_2$ or

735    seawater

736    •    Diffusion and transport-controlled phenomena could cause a pronounced weakening

737    when it comes to seawater and $MgCl_2$ brine

738    •    Creep strain induced by exposure to seawater or $MgCl_2$ occurred at greater rates during

739    periods of bypass than flooding

740    •    Dissolution of chalk grains solely or together with precipitation (or re-precipitation)

741    should be taken into account in the field of water weakening of chalk

742 • Flooding rate plays an important role in the changing of the time dependent behavior of

743 chalk

750 ABBREVIATIONS

751 SSW, synthetic seawater; SSW-1[$Mg^{2+}$], synthetic seawater without magnesium; DW, distilled

752 water.

753 REFERENCES

754 Allen, D. R., Mayuga, M. N. (1970) *"*Subsidence in the Wilmington oilfield, Long Beach,

755 California." *U.S.A. Land Subsidence Sym., Int. Ass. Sci. Hydrol. & UNESCO*, 66-87.

756 Andersen, M. A., Foged, N., Pedersen, H. F. (1992) "The rate-type compaction of a weak

757 North Sea chalk." *33$^{rd}$ U.S. Rock Mech. Sym.,* Santa Fe, New Mexico.

758 Brignoli, M., Santarelli, F. J., Righetti, C. (1994) "Capillary phenomena in impure chalk."

759 *EUROCK'94,* Delf, The Netherlands.

760 Cathles, L. M. (2006) "EQAlt-Equilibrium Chemical Alteration. Combined Physical and

761 Chemical Geofluids Modelling." University of Winsdor, Ontario, Canada.

762     Chin, L. Y., Boade, R. R., Nagel, N. B., Landa, G.H. (1994) "Numerical simulation of Ekofisk

763     reservoir compaction and subsidence: Treating the mechanical behavior of the overburden and

764     reservoir." *2nd SPE/ISRM Rock Mech. In Petrol. Eng. (EUROCK 94), Int. Conf.* Delft, The

765     Netherland., 787-794.

766     De Gennaro, V., Delage, P., Cui, Y. J., Schroeder, Ch., Collin, F. (2003) "Time-dependent

767     behavior of oil reservoir chalk: a multiphase approach." *Soils and Foundations,* 43(4): 131-148.

768     Delage, P., Schroeder, C., Cui, Y. J. (1996) "Subsidence and capillary effects in chalks."

769     *Eurock'96,* Balkema, Rotterdam, The Netherlands.

770     Dusseault, M. B. (1983) "Identifying reservoirs susceptible to subsidence due to fluid

771     withdrawal." *Subsidence Due to Fluid Withdrawals Forum,* Checotah, Okla. U.S. Dept. Energy

772     & Venez Min Energy Mines, 6-14.

773     Ellis, A. (1963) "The solubility of calcite in sodium chloride solutions at high temperatures."

774     *Am. J. Sci.,* 261: 259-267.

775     Fredrich, J. T., Arguello, J. G., Thorne, B. J., Wawersik, W. R., Deitrick, G. L., De Rouffignac,

776     E. P., Myer, L. R., Bruno, M. S. (1996) "Three-dimensional geomechanical simulation of

777     reservoir compaction and implications for well failures in the Belridge Diatomite." *Annul. SPE*

778     *Tech. Conf.,* Denver U.S., 195-210.

779     Gauer, P. R., Sylte, J. E. Nagel, N. B. (2002) "Ekofisk field well log decompaction."

780     *SPE/ISRM Rock Mech. Conf.,* SPE/ISRM: 78177, Irving TX.

781    Gutierrez, M., Øino, L. E., Høeg K. (2000) "The effect of fluid content on the mechanical

782    behavior of fractures in chalk." *Rock Mech. and Rock Eng.,* 33(2): 93-117.

783    Heggheim, T., Madland, M. V., Risnes, R., Austad, T. (2005) "A chemical induced enhanced

784    weakening of chalk by seawater." J. Petr. Sci. Eng., 46(3): 171-174.

785    Hellmann, R., Renders, P. J. N.; Gratier, J.-P., Guiguet, R. (2002a) "Experimental pressure

786    solution of chalk in aqueous solutions: Part 2. Deformation examined by SEM, porosimetry,

787    synthetic permeability, and X-ray computerized tomography." *Water -Rock Interactions, Ore*

788    *Deposits, and Environmental Geochemistry:* A Tribute to David A. Crerar. The Geochemical

789    Society, Special Publication, 7.

790    Hellmann, R., Renders, P. J. N., Gratier, J.-P., Guiguet, R. (2002b) "Experimental pressure

791    solution of chalk in aqueous solutions: Part 1. Deformation behavior and chemistry." *Water –*

792    *Rock Interactions, Ore Deposits, and Environmental Geochemistry:* A Tribute to David A.

793    Crerar. The Geochemical Society, Special Publication, 7.

794    Hiorth, A., Cathles, L. M., Kolnes, J., Vikane, O., Lohne, A., Korsnes, R. I., Madland, M. V.

795    (2008) "Chemical modeling of wettability change in carbonate rocks." *Wettability Sym,.* Abu

796    Dhabi, UAE.

797    Hiorth, A., Cathles, L. M., Kolnes, J., Vikane, O., Lohne, A., Korsnes, R. I., Madland, M. V.

798    (2008) "A chemical model for the seawater-$CO_2$-carbonate system- aqueous and surface

799    chemistry." *Int. Conf. of Society of Core Analysts,* Abu Dhabi, UAE.

800    Hjuler, M. L. (2007) *Diagenesis of Upper Cretaceous onshore and offshore chalk from the*

801    *North Sea area.* PhD Thesis, Danish Technical University (DTU).

802  Homand, S., Shao, J. F. (2000) "Mechanical behavior of a porous chalk and effect of saturating

803  fluid." *Mech. Cohes.-Frict. Mater.,* 5: 583-606.

804  Hughes, B. (1999) *Fluid fact, Engineering Handbook,* Part Number 008902097. Baker Hughes

805  INTEQ.

806  Kolnes, J., Hiorth, A., Siqveland, O. K., Omdal, E., Zangiabadi, B., Madland, M. V. (2008)

807  "Contact angle measurement on calcite using model oils" *Wettability Sym.,* Abu Dhabi, UAE.

808  Korsnes, R. I. (2007) *Chemical induced water weakening of chalk by fluid-rock interactions, a*

809  *mechanistic study.* PhD Thesis, University of Stavanger (UiS), Stavanger.

810  Korsnes, R. I., Madland, M. V., Austad, T., Haver, S., Røsland, G. (2008) "The effects of

811  temperature on the water weakening of chalk by seawater." *J. Petr. Sci. Eng.,* 60(3-4): 183-193.

812  Madland, M. V., Hiorth, A., Korsnes, R.I., Evje, S., Cathles, L. (2009) "Rock fluid interaction

813  in chalk exposed injection of seawater, $MgCl_2$, and NaCl Brines with equal ionic strength." *15$^{th}$*

814  *European Sym. on improved oil recovery,* Paris, France.

815  Madland, M. V., Midtgarden, K., Manafov, R., Korsnes, R. I., Kristiansen, T. G., Hiorth, A.

816  (2008) "The effect of temperature and brine composition on the mechanical strength of Kansas

817  chalk." *Int. Sym. of the Society of Core Analysts (SCA),* Abu Dhabi, UAE.

818  Maury, V., Piau, J. M., Halle, G. (1996) "Subsidence induced by water injection in water

819  sensitive reservoir rocks: the example of Ekofisk." *5$^{th}$ North Sea chalk Sym.,* Reims, France.

820  Millero, F. J., Milne, P. J., Thurmond, V. L. (1984) "The solubility of calcite, strontianite and

821  witherite in NaCl solutions at 25°C." *Geochimica et Cosmochimica Acta.,* 48(5): 1141-1143.

822    Mucci, A. (1983) "The solubility of calcite and aragonite in seawater at various salinities

823    temperatures, and one atmosphere total pressure." *Am. J. Sci.,* 283: 780-799.

824    Nagel, N. B., (2001) "Compaction and subsidence issues within the petroleum industry: from

825    Wilmington to Ekofisk and beyond." *Phys. Chem. Earth (A).,* 26(1-2): 3-14.

826    Newman, G. H. (1983) "The effect of water chemistry on the laboratory compression and

827    permeability characteristics of some North Sea chalks." *J. Petr. Tech.,* 35(5): 976-980.

828    Papamichos, E., Brignoli, M., Santerelli, F. J., (1997) "An experimental and theoretical study

829    of partially saturated collapsible rocks." *Mech. Cohes.-Frict. Mater.,* 2: 251-278.

830    Pierre, A., Lamarche, J. M., Mercire, A., Foissy, A., Persello, J. (1990) "Calcium as potential

831    determining ion in aqueous calcite suspensions." *J. Dispersion Sci. & Tech.,* 11(6): 611-635.

832    Plischke, B. (1996) "Some aspects of numerical simulation of water-induced chalk

833    compaction." *5th North Sea Chalk Sym.,* Reims, France.

834    Powell, B. N., Lovell, G.L. (1994) "Mechanisms of chalk compaction." *SPE/ISRM Rock Mech.*

835    *in Petrol. Eng. Conf.,* Delf, The Netherlands.

836    Pratt, W. E., Johnson, D.W. (1926) "Local subsidence of the Goose Creek oilfield." *J. Geol.,*

837    34: 577-590.

838    Puntervold, T., Strand, S., Austad, T. (2007) "New method to prepare outcrop chalk cores for

839    wettability oil recovery studies at low initial water saturation." *Energy & Fuels.,* 21: 3425-3430.

840      Rezaei Gomari, K. A., Hamouda, A. A., Denoyel, R. (2006) "Influence of sulfate ions on the

841      interaction between fatty acids and calcite surface." *Colloids and Surfaces A: Physicochem. Eng.*

842      *Aspects.,* 287(1-3): 29-35.

843      Risnes, R. (2001) "Deformation and yield in high porosity outcrop chalk." *Phys. Chem. Earth*

844      *(A).,* 26(1-2): 53-57.

845      Risnes, R., Flaageng, O. (1999) "Mechanical properties of chalk with emphasis on chalk– fluid

846      interactions and micromechanical aspects." *Oil Gas Sci. Tech. IFP,* 54(6): 751-758 (Éditions

847      Technip).

848      Risnes, R., Haghighi, H., Korsnes, R.I., Natvik, O. (2003) "Chalk–fluid interactions with

849      glycol and brines." *Tectonophysics,* 370: 213-226.

850      Ruddy, I., Anderson, M.A., Pattillo. P.D., Bishlawi, M., Foged, N. (1998) "Rock

851      compressibility, compaction, and subsidence in a high-porosity chalk reservoir: a case study of

852      Valhall field." 63rd *Annul. SPE Tech. Conf.,* Houston, 179-186.

853      Ruiz-Agudo, E., Putnis, C.V., Jiménez-López, C., Rodriguez-Navarro C. (2009) "An atomic

854      force microscopy study of calcite dissolution in saline solutions: The role of magnesium ions."

855      *Geochimica et Cosmochimica Acta.,* 73(11): 3201-3217.

856      Schoonbeek, J. B. (1977) "Land subsidence as a result of gas extraction in Groningen." The

857      Netherlands, *2nd Int. land subsidence Sym.,* Anaheim, Calif., 267-284.

858      Schroeder, C., Shao, J. F. (1996) "Plastic deformations and capillary effects in chalks." *5th*

859      *North Sea chalk Sym.,* Reims, France.

860    Segnit, E. R., Holland, H. D., Biscardi, C. J. (1962) "The solubility of calcite in aqueous

861    solutions -I: The solubility of calcite in water between 75 and 200 °C at $CO_2$ pressures up to 60

862    atm." *Geochimica et Cosmochimica Acta.,* 26: 1301-1331.

863    Smith, D. J. (1988) "Project management of subsidence and Ekofisk jacking project." *20th*

864    *Annu. SPE Offshore Tech. Conf.,* (OTC 88), Houston TX, 341-368.

865    Spencer, A. M., Briskeby, P. I., Christensen, L. D., Foyn, R., Kjølleberg, M., Kvadsheim, E.,

866    Knight, I., Larsen, M. R., Williams, J. (2008) "Petroleum geoscience in Norden – exploration,

867    production and organization." *Episodes,* 31, 115-124.

868    Strand, S., Høgnesen, E. J., Austad, T. (2006) "Wettability alteration of carbonates-effects of

869    potential determining ions ($Ca^{2+}$ and $SO_4^{2-}$) and temperature." *Colloids and Surfaces A:*

870    *Physicochem. Eng. Aspects.,* 275: 1-10.

871    Sulak, R. M. (1990) "Ekofisk field: The first 20 years." *65th Annual SPE Tech. Conf.,* New

872    Orleans, LA., 521-529.

873    Zangiabadi, B., Korsnes, R.I., Hildebrand-Habel, T., Hiorth, A., Sutarjana, I.K., Lian, A.,

874    Madland, M.V. (2009) "Chemical water weakening of various outcrop chalks at elevated

875    temperature." In: H.I. Ling, Smyth, A., and Betti, R. (Editor), *4th Biot conference on*

876    *poromechanics.* DEStech Publication Inc. Columbia University, New York, 543-548.

877    Zangiabadi, B., Kulathilagon P., Midtun, B. (2011) "Evaluation of rock-fluid interactions in an

878    outcrop chalk: Experimental study with $MgCl_2$ solution." *45th US Rock Mech. Sym., 4th U.S.-*

879    *Canada Rock Mech. Sym.,* Asheville, NC.

880    Zhang, X., Spiers, C. J. (2005) "Compaction of granular calcite by pressure solution at room

881    temperature and effects of pore fluid chemistry." *Int. J. Rock. Mech. Mining Sci.,* 42: 950-960.

882

883 **Table 1.** Brine composition; M = molar

| Brine \\ Salts (g/l)) | 0.657 M NaCl | 0.657 M NaCl with tracer | 0.219 M Na$_2$SO$_4$ | 0.219 M Na$_2$SO$_4$ with tracer | 0.219 M MgCl$_2$ | 0.110 M MgCl$_2$ | 0.219 M CaCl$_2$ | SSW-1[Mg$^{2+}$] | SSW |
|---|---|---|---|---|---|---|---|---|---|
| LiCl (Li$^+$: tracer) | | 1.02 | | | | | | | |
| NaCl | 38.40 | 38.40 | | | | | | 27.62 | 23.38 |
| Na$_2$SO$_4$ | | | 31.1 | 31.1 | | | | 3.41 | 3.41 |
| KSCN (SCN$^-$: tracer) | | | | 2.33 | | | | | |
| NaHCO$_3$ | | | | | | | | 0.17 | 0.17 |
| KCl | | | | | | | | 0.75 | 0.75 |
| MgCl$_2$+ 6 H$_2$O | | | | | 44.5 | 22.25 | | | 9.05 |
| CaCl$_2$ + 2 H$_2$O | | | | | | | 32.2 | 1.91 | 1.91 |

884

885 **Table 2.** Experimental observations for cores in different aqueous solutions during loading phase

| Core no. | Brine | Porosity [%] | | Yield [MPa] | | Bulk modulus [GPa] | | Creep stress level [MPa] | | Total strain within loading [%] | |
|---|---|---|---|---|---|---|---|---|---|---|---|
| Group 1: First phase; Flooding, second phase; Bypass | | | | | | | | | | | |
| SK3 | DW | 43.90 | | 7.7 | | 1.1 | | 10.5 | | 0.80 | |
| SK8 | NaCl | 45.10 | | 6.2 | | 0.50 | | 9.4 | | 1.33 | |
| SK2 | Na$_2$SO$_4$ | 45.20 | | 4.6 | | 0.32 | | 7.7 | | 2.20 | |
| SK1 | MgCl$_2$ | 45.76 | | 5.0 | | 0.71 | | 7.3 | | 1.4 | |
| SK26 | CaCl$_2$ | 45.63 | Avg. 46.15 | 5.2 | Avg. 4.95 | 0.52 | Avg. 0.54 | 6.6 | | 0.68 | Avg. 0.73 |
| SK28 | | 46.68 | | 4.7 | | 0.55 | | | | 0.77 | |
| SK16 | SSW-1[Mg$^{2+}$] | 47.12 | | 4.7 | | 0.57 | | 7.9 | | 1.16 | |
| Group 2: First phase; Bypass, second phase; Flooding | | | | | | | | | | | |
| SK6 | Na$_2$SO$_4$ | 45.1 | | 4.9 | Avg. 4.85 | 0.37 | | 7.7 | Avg. 7.65 | 1.9 | Avg. 2.25 |
| SK5 | | 45.4 | | 4.8 | | | | 7.6 | | 2.6 | |

| Core no. | Brine | | | | | | | | | | |
|---|---|---|---|---|---|---|---|---|---|---|---|
| SK7 | $MgCl_2$ | 45.5 | | 5.7 | | 0.46 | | 8.8 | | 1.82 | |
| SK4 | SSW-1[$Mg^{2+}$] | 44.55 | Avg. 45.20 | 5.7 | Avg. 4.85 | 0.64 | Avg. 0.5 | 8.9 | Avg. 7.9 | 0.81 | Avg. 1.17 |
| SK11 | | 45.84 | | 4.0 | | 0.36 | | 6.9 | | 1.52 | |
| SK17 | SSW | 46.01 | | 4.8 | | 0.42 | | 7.4 | | 2.7 | |

886

**Table 3.** Experimental observations for cores in different aqueous solutions during creep stage

| Core no. | Brine | Creep stress level [MPa] | Total creep strain [%], end of $1^{st}$ phase | | Total creep strain [%], end of $2^{nd}$ phase | | Strain rate [%/time decade], first phase | | Strain rate [%/time decade], second phase | |
|---|---|---|---|---|---|---|---|---|---|---|
| Group 1: First phase; Flooding (a week), second phase; Bypass (a week) | | | | | | | | | | |
| SK3 | DW | 10.5 | 0.15 | | - | | 0.06 | | - | |
| SK8 | NaCl | 9.4 | 1.25 | | 1.33 | | 0.45 | | 0.45 | |
| SK2 | $Na_2SO_4$ | 7.7 | 1.83 | | 2.23 | | 1.21 | | 1.21 | |
| SK1 | $MgCl_2$ | 7.3 | 0.84 | | 1.25 | | 0.3 | | 1.7 | |
| SK26 | $CaCl_2$ | 6.6 | 1.05 | Avg. 0.93 | - | | 0.35 | Avg. 0.45 | - | |
| SK28 | | | 0.8 | | - | | 0.55 | | - | |
| SK16 | SSW-1[$Mg^{2+}$] | 7.9 | 1.84 | | 2.34 | | 1.43 | | 1.43 | |
| Group 2: First phase; Bypass (a week), second phase; Flooding (a week) | | | | | | | | | | |
| SK5 | $Na_2SO_4$ | 7.6 | 1.5 | | 1.72 | | 0.5 | | 2.9 | |
| SK7 | $MgCl_2$ | 8.8 | 1.19 | | 1.27 | | 0.84 | | 0.37 | |
| SK4 | SSW-1[$Mg^{2+}$] | 8.9 | 1.18 | Avg. 1.18 | 2.25 | Avg. 2.05 | 0.46 | Avg. 0.46 | 2.8 | Avg. 2.55 |
| SK11 | | 6.9 | 1.18 | | 1.85 | | 0.46 | | 2.3 | |
| SK17 | SSW | 7.4 | 2.00 | | 2.33 | | 2.15 | | 0.85 | |

888

889　　**Table 4.** Experimental observations for cores: initially saturated and flooded with distilled water

890　　and changed to saline solutions

| Core no. | Brine (switched within creep phase) | Porosity [%] | Yield [MPa] | Strain rate within flooding DW [%/time decade] | Strain rate within flooding brine [%/time decade] |
|---|---|---|---|---|---|
| SK20 | DW → NaCl | 45.05 | 6.5 | 0.22 | 2.5 |
| SK5A | DW → $Na_2SO_4$ | 51.17 | 6.7 | 0.5 | 1.21 |

891

892
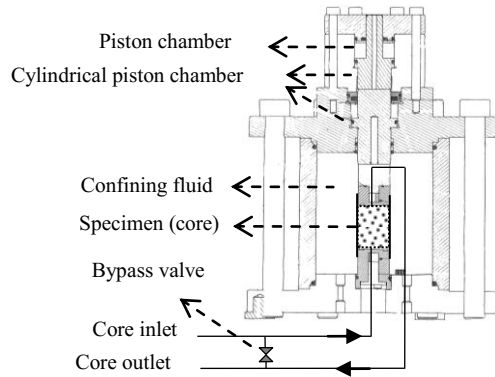
**Figure 1.** Schematic illustration of triaxial cell, including flooding and bypass line
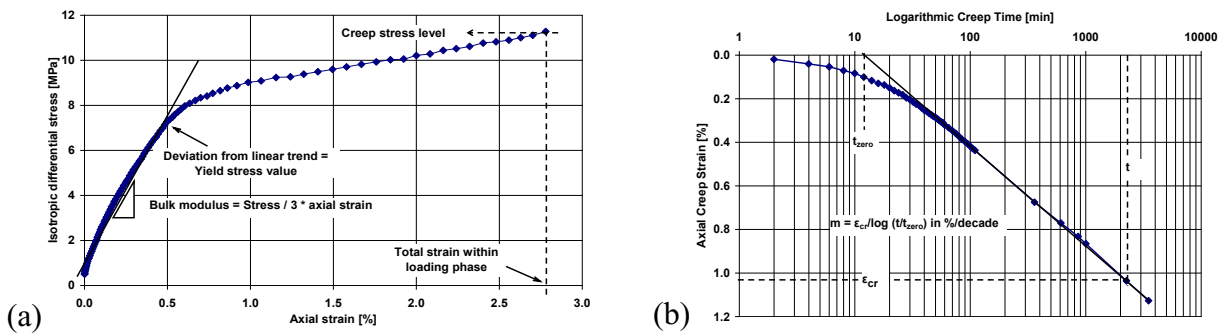


894 **Figure 2.** (a) Schematic diagram of hydrostatic loading phase, yield stress value, total strain

895 within loading phase, and creep stress level;  (b) Schematic diagram of creep phase in semi-

896 logarithmic, creep strain slope (m)
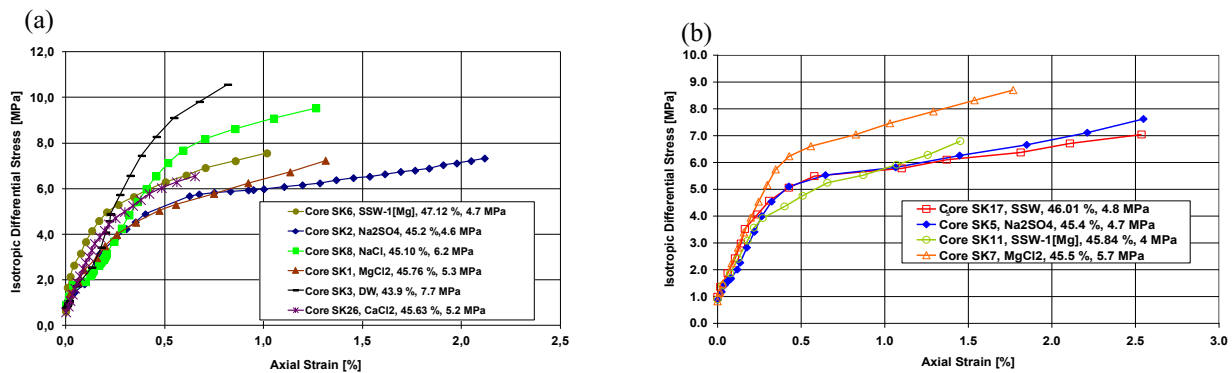


897 **Figure 3.** (a) Hydrostatic compression tests on flooded cores. Legend: brine, porosity, yield

898 stress value; (b) Hydrostatic compression tests on flood-bypassed cores bypassed. Legend: brine,

899 porosity, yield stress value

47
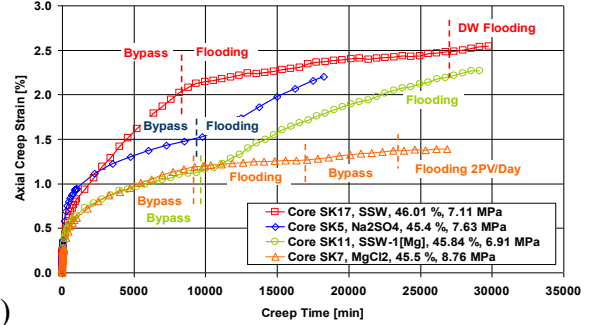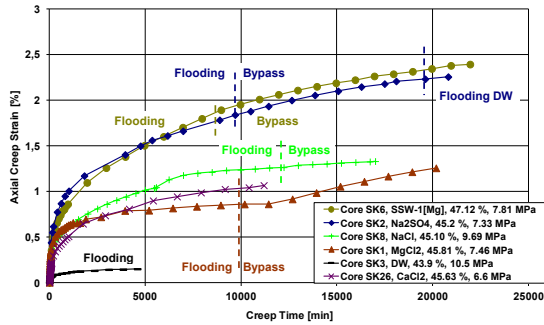
**Figure 4.** (a) Axial creep strain vs. creep time, first week saturated and then flooded, Legend: core number, brine, porosity, creep stress level; (b) Axial creep strain vs. creep time, first week bypassed and then flooded, Legend: brine, porosity, stress level
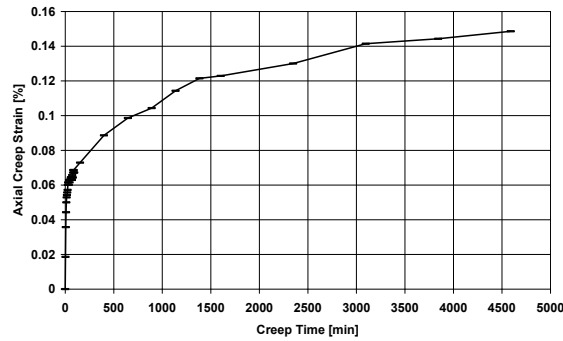


**Figure 5.** Axial creep strain vs. creep time for core SK3 flooded with distilled water, Stress level = 10.5 MPa
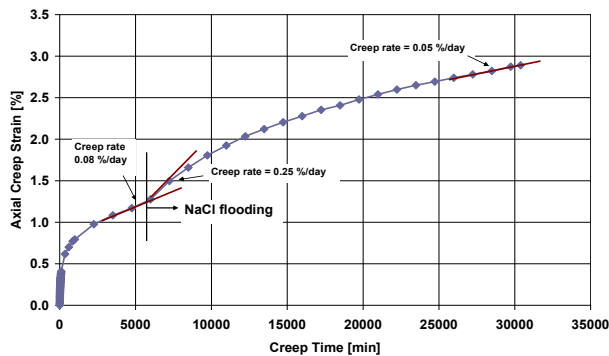


**Figure 6.** Axial creep strain vs. creep time for core SK20 flooded with DW followed by 0.657 M NaCl brine; Stress level = 9.3 MPa
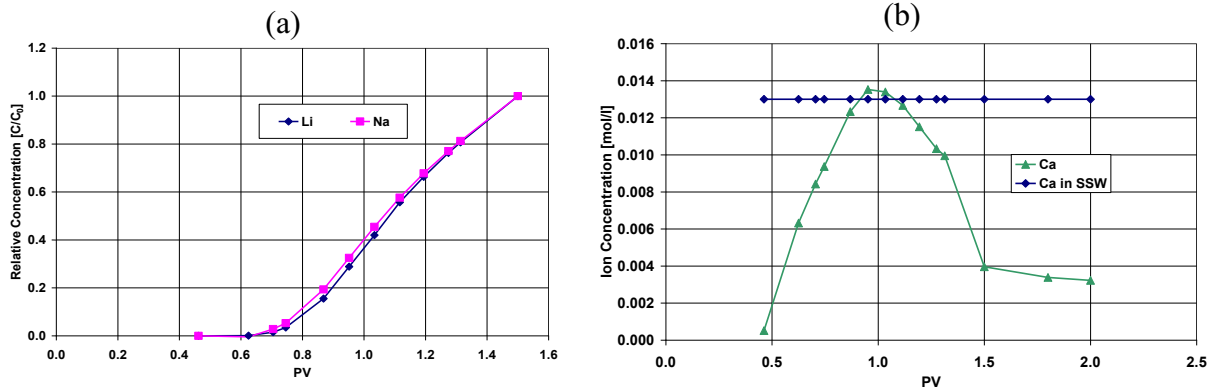
Figure 7. (a) Relative concentration of $Li^+$ and $Na^+$ ions at the core outlet, core SK20, flooded with 0.657 M NaCl. Small area between two cation curves is due to little adsorption of sodium in the core. (b) Calcium concentration in analyzed effluents after NaCl injection, core SK20
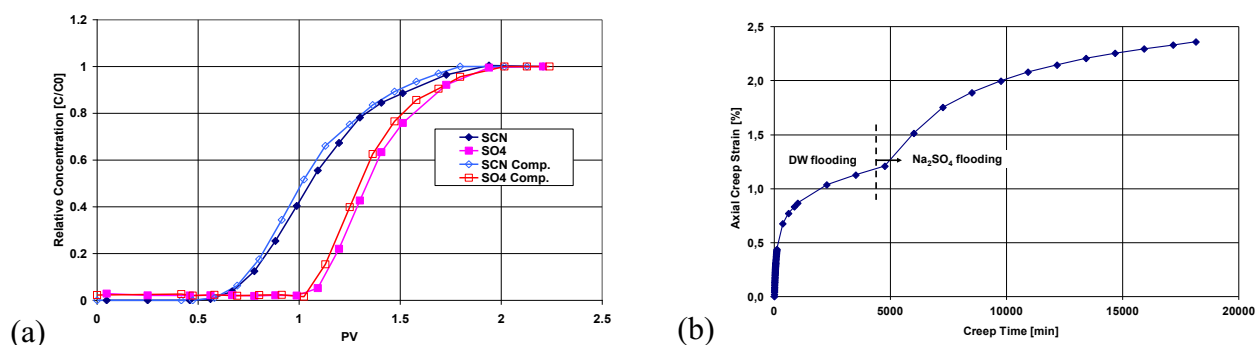


Figure 8. (a) Relative concentrations of $SCN^-$ and $SO_4^{2-}$ at the core outlet, core SK5A, flooded with 0.219 M $Na_2SO_4$ brine with tracer Comp.: compacted core after hydrostatic loading. (b) Axial creep strain vs. logarithmic creep time for core SK5A; Stress level = 8.2 MPa



49
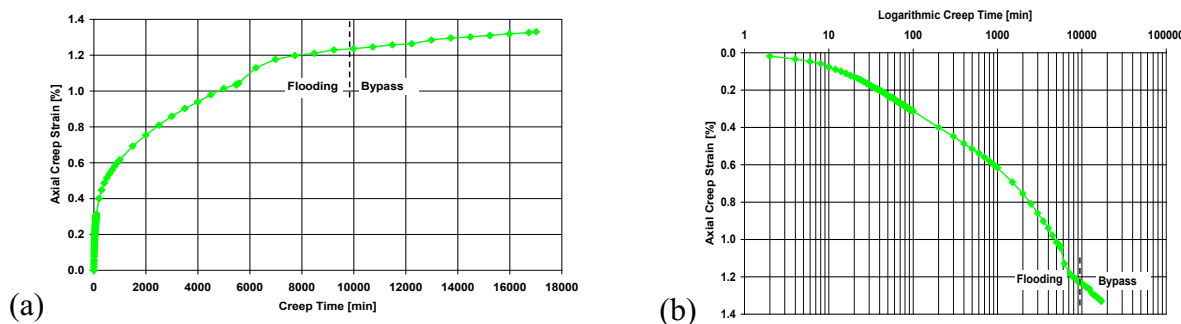
913     **Figure 9.** (a) Axial creep strain vs. creep time for core SK8, Stress level = 9.6 MPa; Saturation

914     brine: NaCl (b) Axial creep strain vs. logarithmic creep time for core SK8, Stress level = 9.6

915     MPa; Saturation brine: NaCl



(a)                                                          (b)
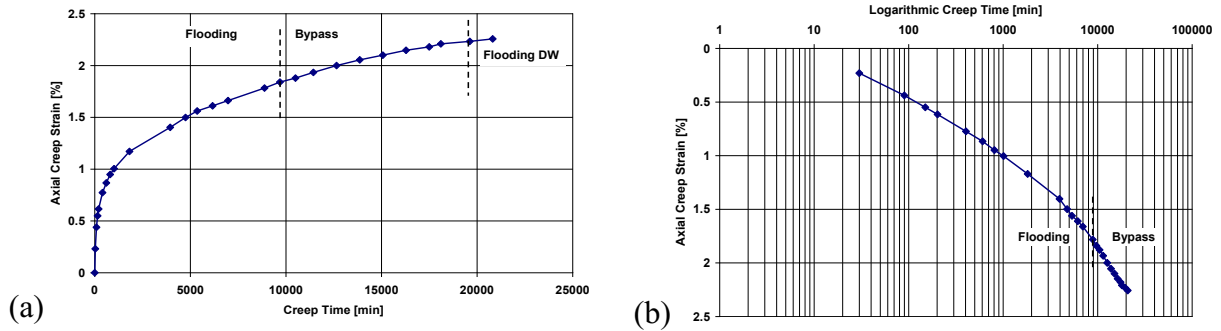
916     **Figure 10.** (a) Axial creep strain vs. creep time for core SK2; Stress level = 7.4 MPa; Saturation

917     brine: $Na_2SO_4$ solution (b) Axial creep strain vs. logarithmic creep time for core SK2; Stress

918     level = 7.4 MPa; Saturation brine: $Na_2SO_4$ solution
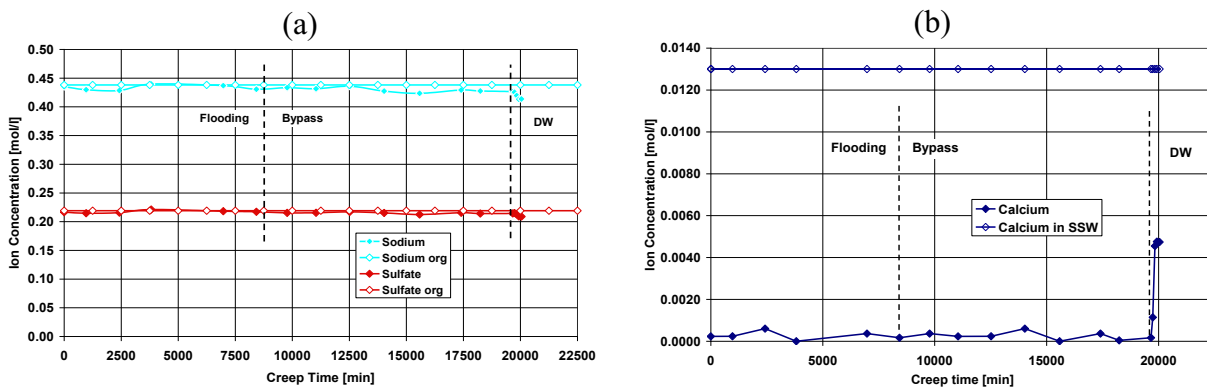


919     **Figure 11.** (a) Chemical analysis result for $Na^+$ and $SO_4^{2-}$ ions in sampled effluent of core SK2

920     flooded with 0.219 M $Na_2SO_4$. The original concentrations (sodium org, sulfate org) are included

921     for comparison; (b) Chemical analysis result for $Ca^{2+}$ ions in sampled effluent of core SK2

922     flooded with 0.219 M $Na_2SO_4$. The concentration of calcium in SSW is included for comparison.
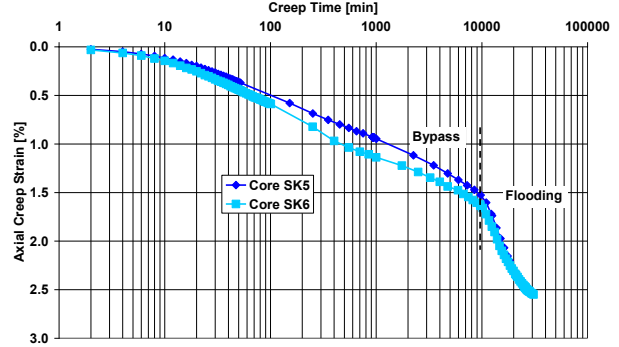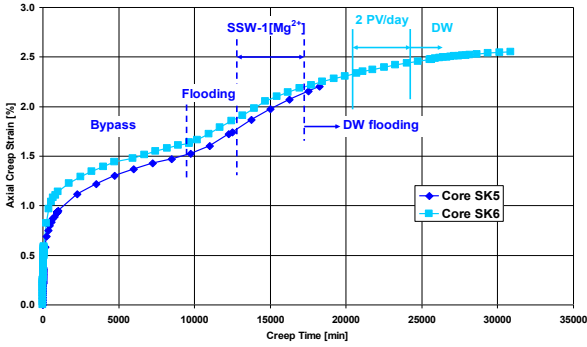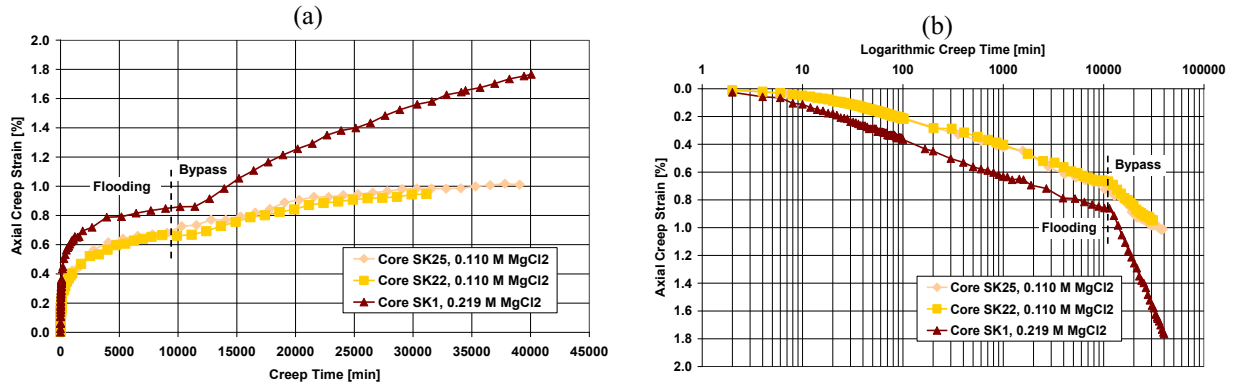
923    **Figure 12.** (a) Axial creep strain vs. creep time for cores SK5 and SK6; Stress level = 7.6 and

924    7.5 MPa; (b) Axial creep strain vs. logarithmic creep time for core SK5 and SK6; Stress level =

925    7.6 and 7.5 MPa.
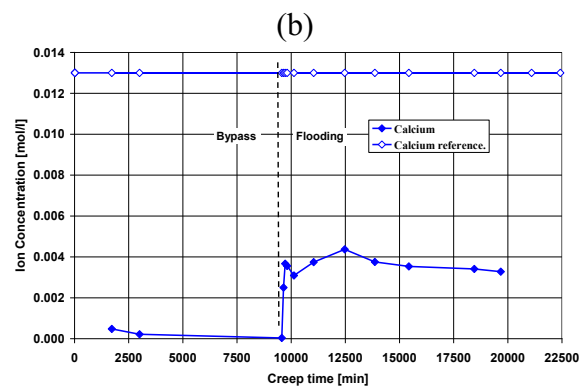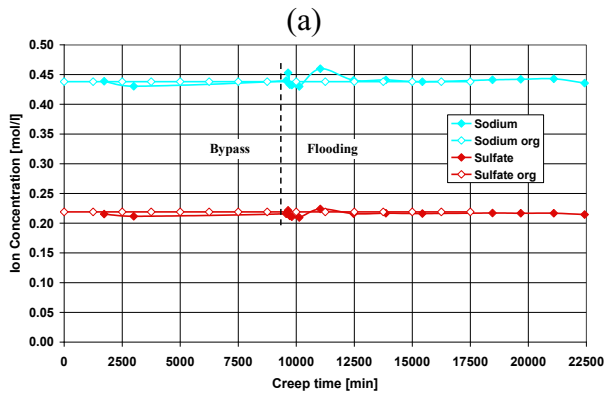


926    **Figure 13.** (a) Chemical analysis result for $Na^+$ and $SO_4^{2-}$ ions in sampled effluent of core SK6

927    flooded with 0.219 M $Na_2SO_4$. The original concentrations (sodium org, sulfate org) are included

928    for comparison; (b) Chemical analysis result for $Ca^{2+}$ ions in sampled effluent of core SK6

929    flooded with 0.219 M $Na_2SO_4$. The concentration of calcium is included for comparison.



51
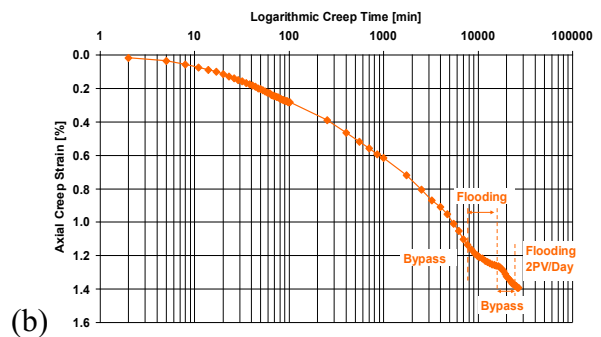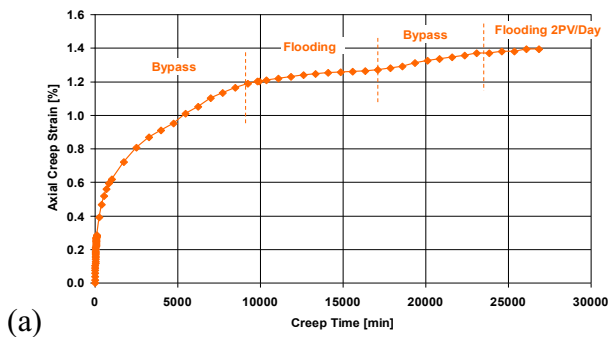
930    **Figure 14.** (a) Axial creep strain vs. creep time for core SK7; Stress level = 9.2 MPa; Saturation

931    brine: MgCl$_2$ solution (b) Axial creep strain vs. logarithmic creep time for core SK7; Stress level

932    = 9.2 MPa; Saturation brine: MgCl$_2$ solution
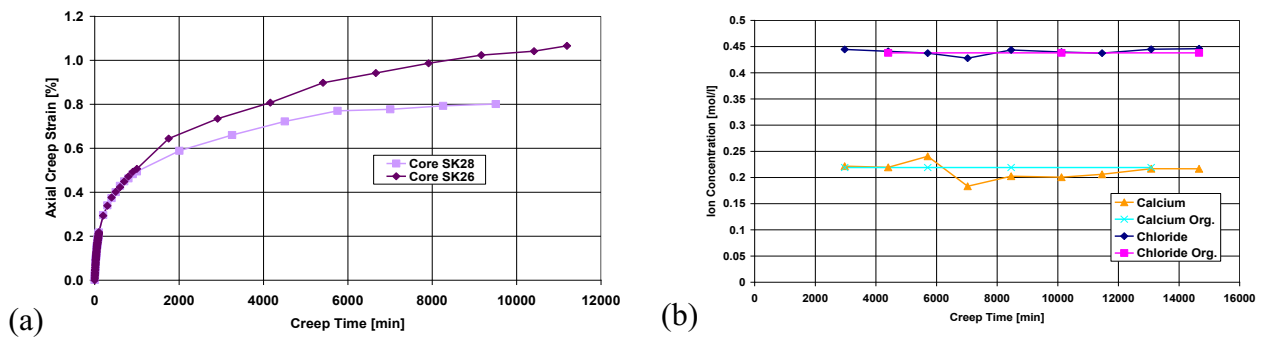


933    **Figure 15.** (a) Axial creep strain vs. creep time for core SK1, SK22, and SK25; Stress level =

934    7.4, 11, and 10.1 MPa ; (b) Axial creep strain vs. logarithmic creep time for core SK1, SK22, and

935    SK25; Stress level = 7.4, 11, and 10.1 MPa
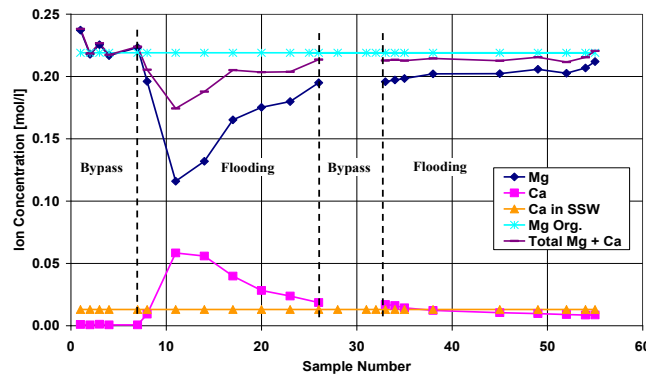


936    **Figure 16.** Concentration of Mg$^{2+}$ + Ca$^{2+}$ ions in the sampled effluents of core SK7, flooded with

937    0.219 M MgCl$_2$; Org.: Original concentration

Grain
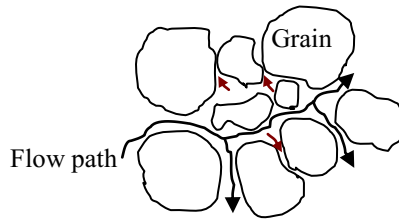
Flow path

938  **Figure 17.** Schematic illustration of the flow path of MgCl$_2$ brine in chalk; Black arrows;

939  flooding pathway, brown arrows: probable pathways within the bypass period



(a)



(b)

940  **Figure 18.** (a) Axial creep strain vs. creep time for cores SK26 and SK28; Stress level = 6.6

941  MPa; (b) Concentration of Ca$^{2+}$ and Cl$^-$ in sampled effluents (sampling started from beginning of

942  creep stage), core SK26, flooded with 0.219 M CaCl$_2$. Org.: Original concentration
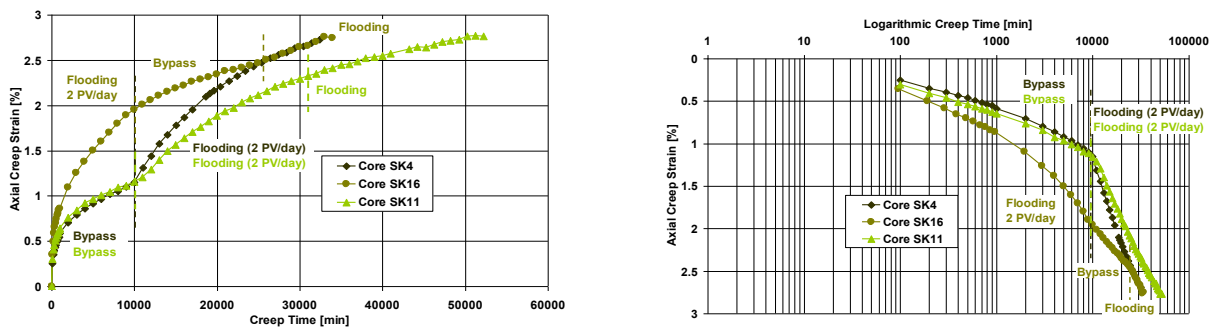




943  **Figure 19.** (a) Axial creep strain vs. creep time for cores SK4, SK16, and SK11; Stress level = 9,

944  7.9 and 6.9 MPa; Saturation brine: seawater without magnesium (SSW-1[Mg$^{2+}$]); (b) Axial creep

945  strain vs. logarithmic creep time for cores SK4, SK16, and SK11; Stress level = 9, 7.9 and 6.9

946  MPa. Saturation brine: seawater without magnesium (SSW-1[Mg$^{2+}$])